



**STRUCTURAL SYSTEMS
RESEARCH PROJECT**



PB99-106411

Report No.
SSRP - 97/12

**THE INFLUENCE OF MEMBER SIZE ON
THE SHEAR RESPONSE OF
REINFORCED CONCRETE MEMBERS**

by

MICHAEL P. COLLINS

Final Report on a Research Project funded by Caltrans under
Contract No. 59V375

August 1997

Division of Structural Engineering
University of California, San Diego
La Jolla, California 92093-0085

Memorandum

To: JAMES E. ROBERTS, Director
Engineering Service Center

Date: August 21, 1998
File: 59V375-Area 2
Report SSRP-97/12
900.17

From: DEPARTMENT OF TRANSPORTATION
Engineering Service Center
Office of Earthquake Engineering and Design Support

Subject: Final Report for Caltrans "Problem Focused Study" Project Titled:

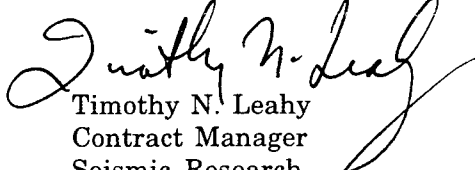
**"The Influence of Member Size on The Shear Response
Reinforced Concrete Members"**

The attached report was completed as part of the proposed work in contract #59-V-375, a Research Technical Agreement between Caltrans and the University of California, San Diego, for the project titled; "Coordinated Seismic Bridge Research Program at the University of California, San Diego" The author is Michael P. Collins. The report number is "UCSD/SSRP-97/12". This is the fourth final report of 5 that has been produced as the product of "Area 2 of 3" of the contract; and is one of 11 reports that will be produced from this contract.

The primary goal of this part of the research study was to investigate seismic performance of bridge columns.

The total contract cost was \$1,427,000, and the original performance period was August 1, 1993 thru January 31, 1996. Amendment #1 extended the termination to March 31, 1997. There will be 11 final reports delivered from this contract with an executive overview report.

The conclusions of this report begin on page 48. These conclusions include a discussion on the sensitivity of member size effect on shear; and as stated on page 50 : "...provides guidance as to when serious consideration needs to be given to the effects of member size..."


Timothy N. Leahy
Contract Manager
Seismic Research

Attach

cc: JAllison, ESC Deputy Director
CT Hdqrts Library
TRC
Design Sections (14 copies)
Office Chiefs (except noted)
Seismic Seniors & Specialists
Other State contact list

1. Report No. SSRP 97/12	2. Government Accession No.	3. Recipient's Catalog No.	
4. Title and Subtitle The Influence of Member Size on the Shear Response of Reinforced Concrete Members		5. Report Date August 1997	
		6. Performing Organization Code	
7. Author(s) Michael P. Collins		8. Performing Organization Report No. UCSD / SSRP-97/12	
9. Performing Organization Name and Address Division of Structural Engineering School of Engineering University of California, San Diego La Jolla, California 92093-0085		10. Work Unit No. (TRAIS)	
		11. Contract or Grant No. DOT 59V375 - Area 2 of 3	
12. Sponsoring Agency Name and Address California Department of Transportation Engineering Service Center 1801 30 th St., West Building MS-9 Sacramento, California 95807		13. Type of Report and Period Covered Final Report - 4 of 5	
		14. Sponsoring Agency Code 59-304-910R01	
15. Supplementary Notes Prepared in cooperation with the State of California Department of Transportation.			
16. Abstract This report is the 4 th of 5 reports in a series of reports on the seismic performance of columns. When a series of geometrically similar reinforced concrete members fail in shear, the shear stress at failure sometimes substantially decreases as the size of the member increases. Identifying those situations where this size effect in shear is significant is the main objective of the analytical and experimental studies summarized in this report. It is concluded that the columns which contain only small amounts of shear reinforcement, are subjected to low axial loads, and have ratios of column height to member thickness greater than about 2.5, are particularly sensitive to the size effect in shear. The report demonstrates that analytical methods based on the modified compression field theory are capable of predicting reasonably well the magnitude of the size effect in shear.			
17. Key Words concrete, seismic design, bridges, columns, shear		18. Distribution Statement Unlimited	
19. Security Classification (of this report) Unclassified	20. Security Classification (of this page) Unclassified	21. No. of Pages	22. Price

Structural Systems Research Project

Report No. SSRP-97/12

**THE INFLUENCE OF MEMBER SIZE ON THE SHEAR
RESPONSE OF REINFORCED CONCRETE MEMBERS**

by

Michael P. Collins

Visiting Professor

Final Report on a Research Project funded by
Caltrans under Contract No. 59V375

August 1997

PROTECTED UNDER INTERNATIONAL COPYRIGHT
ALL RIGHTS RESERVED.
NATIONAL TECHNICAL INFORMATION SERVICE
U.S. DEPARTMENT OF COMMERCE

ABSTRACT

When a series of geometrically similar reinforced concrete members fail in shear, the shear stress at failure sometimes substantially decreases as the size of the member increases. Identifying those situations where this size effect in shear is significant is the main objective of the analytical and experimental studies summarized in this report. It is concluded that columns which contain only small amounts of shear reinforcement, are subjected to low axial loads, and have ratios of column height to member thickness greater than about 2.5 are particularly sensitive to the size effect in shear. The report demonstrates that analytical methods based on the modified compression field theory are capable of predicting reasonably well the magnitude of the size effect in shear.

ACKNOWLEDGEMENT

The research described in this report was funded by the California Department of Transportation (Caltrans) and by *Concrete Canada*, a Network of Centres of Excellence funded by the Minister of State, Science and Technology, Canada. The author would like to express his gratitude to both of these organizations for their support. The experiments on square reinforced concrete column specimens described in this report, were conducted by Bogdan Stanik and Konstantine Simionopoulos, graduate students at the University of Toronto, as part of their M.A.Sc. theses projects. Their enthusiasm, care and diligence made a significant contribution to the success of the project.

TABLE OF CONTENTS

Abstract	i
Acknowledgement	ii
List of Figures	iv
List of Tables	vi
Notation	vii
1. Introduction	1
2. Modified Compression Field Theory	4
3. The Beta Method for Predicting Shear Strength	15
4. "Column" Tests at the University of Toronto	18
5. Analytical Studies of Column Sections	30
6. Column Tests at the University of California, San Diego	38
7. Conclusions	48
References	51

LIST OF FIGURES

Figure 1.1	Influence of Member Depth and Maximum Aggregate Size on Shear Stress at Failure (Tests by Shioya et al.[1,2])	1
Figure 1.2	Derivation of ACI Expression for Diagonal Cracking Shear V_c (Adapted from Ref. [4])	2
Figure 2.1	Comparison of Calculated and Observed Shear Response of Membrane Element SE6	4
Figure 2.2	A Summary of the Relationships Used in the Modified Compression Field Theory	6
Figure 2.3	Equilibrium of Element SE6 When $\epsilon_1 = 2.5 \times 10^{-3}$ and $\nu = 3.04$ MPa	9
Figure 2.4	Observed Crack Patterns for Element SE6	10
Figure 2.5	Calculation of Crack Spacing Parameters s_x and s_y for Element SE6	11
Figure 2.6	Calculated Values of f_1 for Element SE6	12
Figure 2.7	Influence of Element Size on Predicted Failure Shear Stress of Two Series of Elements Similar to SE6	13
Figure 2.8	Influence of Crack Spacing on the Predicted Shear Strengths of a Series of Elements with Different Amounts of Stirrups	14
Figure 4.1	Details of Specimens Tested at the University of Toronto	19
Figure 4.2	Crack Patterns and Measured Crack Widths (mm) for Specimen WM100D	20
Figure 4.3	Crack Patterns and Measured Crack Widths (mm) for Specimen WM100C	22
Figure 4.4	Crack Patterns and Measured Crack Widths (mm) for Specimen WM30C	26
Figure 4.5	Comparison of Load-Deformation Response of WM100D, WM100C and WM30C	27
Figure 5.1	Influence of Amount of Transverse Reinforcement and Member Size on Predicted Shear Stress at Failure for Members with 1.4% of Longitudinal Steel	31

Figure 5.2	Influence of Amount of Transverse Reinforcement and Member Size on Predicted Shear Stress at Failure for Members with 3% of Longitudinal Reinforcement	32
Figure 5.3	Influence of Axial Load and Member Size on Predicted Shear Stress at Failure	33
Figure 5.4	Influence of Aspect Ratio and Member Size on Predicted Shear Stress at Failure	34
Figure 5.5	Predicted and Observed Strengths of a Series of Reinforced Concrete Beams Tested by Kani	35
Figure 5.6	Strut-and-Tie Models for Columns with Different Aspect Ratios, Showing Member Forces (kN)	36
Figure 6.1	Details of Specimens Tested at University of California, San Diego	39
Figure 6.2	Application of the Beta Method to Circular Cross Sections	41
Figure 6.3	Strut-and-Tie Model of Column L1	43
Figure 6.4	Predicted Load-Deformation Response of Columns L1 and S1-2	45
Figure 6.5	Influence of Crack Spacing on Predicted Load-Deformation Response	46
Figure 6.6	Deformed Shape of L1 under Maximum Load, Predicted by TRIX96	47
Figure 6.7	Crack Pattern for L1 under Maximum Load, Predicted by TRIX96	48

LIST OF TABLES

Table 2.1	Predicted Response of Membrane Element SE6 (Crack spacing parameters: $s_x = 195$ mm; $s_y = 450$ mm)	7
Table 3.1	Values of β and θ for Members Containing at Least the Minimum Amount of Stirrups	16
Table 3.2	Values of β and θ for Members Containing Less than the Minimum Amount of Stirrups	16
Table 4.1	Predicted Shear Capacities of Toronto Columns	30
Table 6.1	Predicted Shear Capacities of San Diego Columns	45
Table 7.1	Comparison of Toronto and San Diego Column Tests	50

NOTATION

- A_{cs} = area of concrete compressive strut
 A_s = area of longitudinal reinforcing bars on flexural tension side of member
 A_v = area of shear reinforcement within distance s
 a = maximum aggregate size
 b_v = effective web width
 b_w = web width
 D_x = diameter of circle through centres of longitudinal bars, circular section
 d = distance from extreme compression fibre to centroid of longitudinal tension reinforcement
 d_b = diameter of reinforcing bar
 d_{beff} = effective bar diameter, bundled bars
 d_{bx} = bar diameter of longitudinal (x) reinforcement
 d_{by} = bar diameter of transverse (y) reinforcement
 d_v = effective shear depth, taken as the flexural lever arm which need not be taken less than $0.9d$.
 E_s = modulus of elasticity of reinforcing bars
 f'_c = compressive strength of concrete
 f_{cr} = cracking strength of concrete
 f_{cu} = limiting concrete stress in compression strut
 f_{sx} = average stress in longitudinal (x) reinforcement
 f_{sxcr} = stress in longitudinal (x) reinforcement, at crack location
 f_{sy} = average stress in transverse (y) reinforcement
 f_{sy-cr} = stress in transverse (y) reinforcement, at crack location
 f_{yield} = yield strength of rebar
 f_{xyield} = yield strength of longitudinal (x) reinforcement
 f_{yyield} = yield strength of transverse (y) reinforcement
 f_1 = average residual tensile stress in cracked concrete
 f_2 = principal compressive stress in concrete
 f_{2max} = crushing strength of diagonally cracked concrete

- h = distance from base of member to point of application of shear force
- M = applied moment, taken as positive
- M_{flex} = pure flexural capacity of section, when axial load is zero and strain hardening of reinforcement is neglected
- N = applied axial load, taken as positive for tension, negative for compression
- n = number of bars in a bundle or number of longitudinal bars around the perimeter of a circular section
- s = spacing of shear reinforcement
- P_u = crushing capacity of concrete compression strut
- s_{maxx} = maximum distance that concrete in the shear area is away from a bar in the longitudinal (x) direction
- s_{maxy} = maximum distance that concrete in the shear area is away from a bar in the transverse (y) direction
- s_x = crack spacing when cracks are perpendicular to the longitudinal (x) reinforcement
- s_y = crack spacing when cracks are perpendicular to the transverse (y) reinforcement
- s_{xe} = equivalent value of s_x for beams in which aggregate size is not 19 mm
- s_θ = crack spacing when cracks are inclined at angle θ to the longitudinal axis of the member
- V = applied shear force
- V_c = shear strength provided by tensile stresses in cracked concrete
- V_{max} = shear strength of section
- v = applied shear stress
- v_c = concrete contribution to the shear resistance
- v_{ci} = shear stress transmitted across a crack
- v_{cimax} = maximum shear stress that can be transmitted across a crack
- v_{max} = maximum shear resistance at a section
- v_s = steel contribution to the shear resistance
- v_u = applied shear stress
- w = crack width

α_s = inclination of concrete compression strut to axis of member
 Δ = lateral displacement
 β = tensile stress factor indicating ability of cracked concrete to transmit shear
 γ_{xy} = average shear strain in x-y plane
 ϵ_1 = principal tensile strain in cracked concrete
 ϵ_2 = principal compressive strain in cracked concrete
 ϵ_c' = strain in concrete when f_c reaches f_c'
 ϵ_x = average longitudinal strain
 ϵ_y = average transverse strain
 ϵ_s = tensile strain in reinforcement crossing strut
 θ = angle of inclination of principal compressive strain in cracked concrete
 with respect to longitudinal axis of member
 ρ = reinforcement ratio
 ρ_ℓ = reinforcement ratio, longitudinal steel
 ρ_w = ratio of transverse web reinforcement
 ρ_x = reinforcement ratio in longitudinal (x) direction
 ρ_y = reinforcement ratio in transverse (y) direction

1. INTRODUCTION

When a series of geometrically similar reinforced concrete members fail in shear, the shear stress at failure sometimes substantially decreases as the size of the member increases. This so-called "size effect in shear" is illustrated in Fig. 1.1, which summarizes the results of an extensive experimental program conducted in Japan by Shioya et al.[1,2] It can be seen that, for these lightly reinforced (0.4% of longitudinal reinforcement, no stirrups), uniformly loaded, simple span beams, the shear stress at failure decreases, both as the member depth increases and as the maximum aggregate size decreases. For these particular beams, increasing the effective depth of the beam from 200 mm to 3 m decreased the shear stress at failure by a factor of about 3.

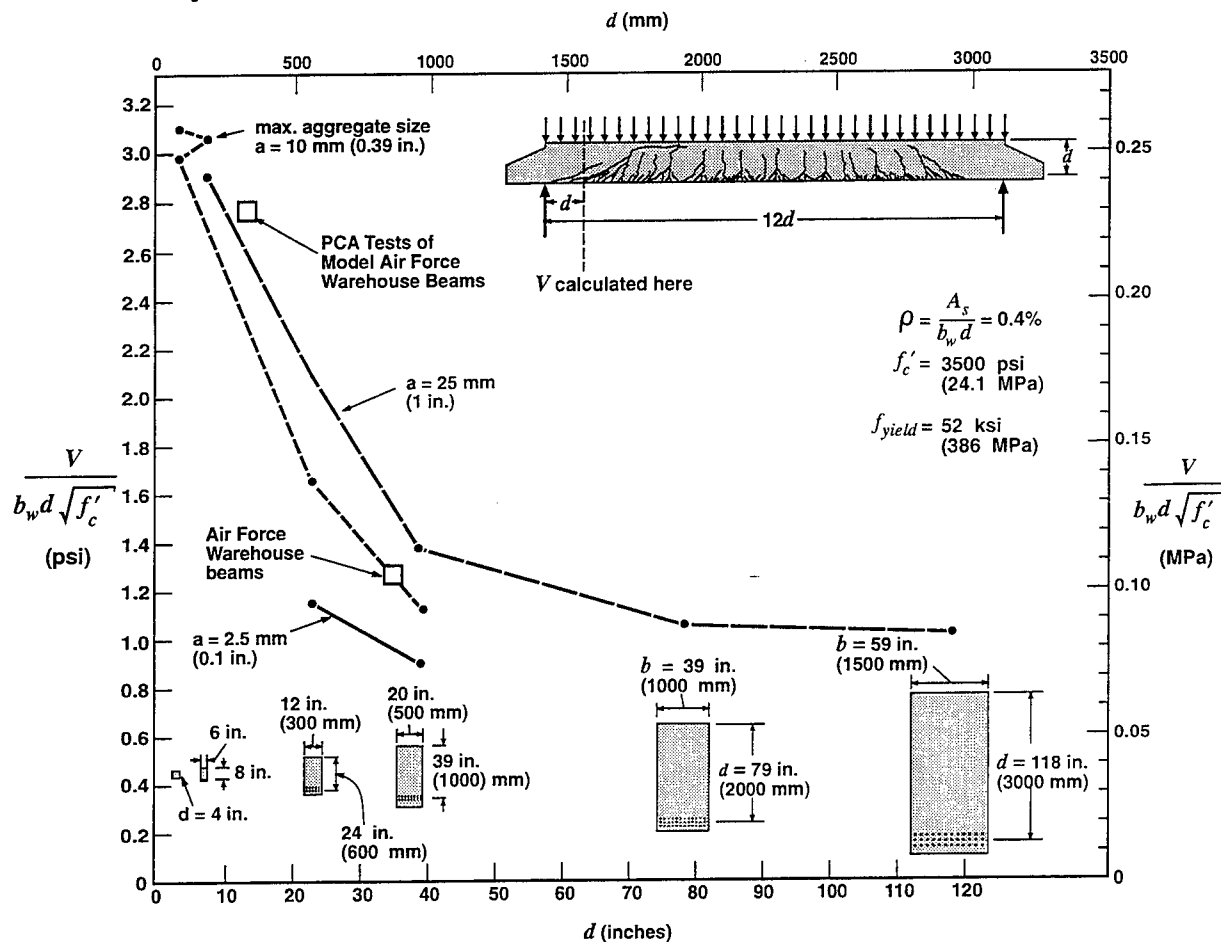


Figure 1.1 Influence of Member Depth and Maximum Aggregate Size on Shear Stress at Failure (Tests by Shioya et al.[1,2])

In the evaluation and design of reinforced concrete structures the engineer uses expressions for shear strength that are typically based on tests of relatively small specimens. For example, the basic ACI[3] expression for the "concrete contribution", V_c , was derived in 1962[4] from the 194 test results shown in Fig. 1.2, where, for MPa units,

$$\begin{aligned} V_c &= 0.158\sqrt{f'_c} b_w d + 17.24\rho_w \frac{Vd}{M} b_w d \\ &\leq 0.291\sqrt{f'_c} b_w d \end{aligned} \quad (1.1)$$

The average depth of these 194 beams was 340 mm, while the average amount of flexural tension reinforcement was 2.2%. The above expression for V_c implies that the shear stress at failure will be greater than $0.158\sqrt{f'_c}$. However, some of the large, lightly reinforced beams shown in Fig. 1.1 failed at shear stresses that were only about 50% of this value.

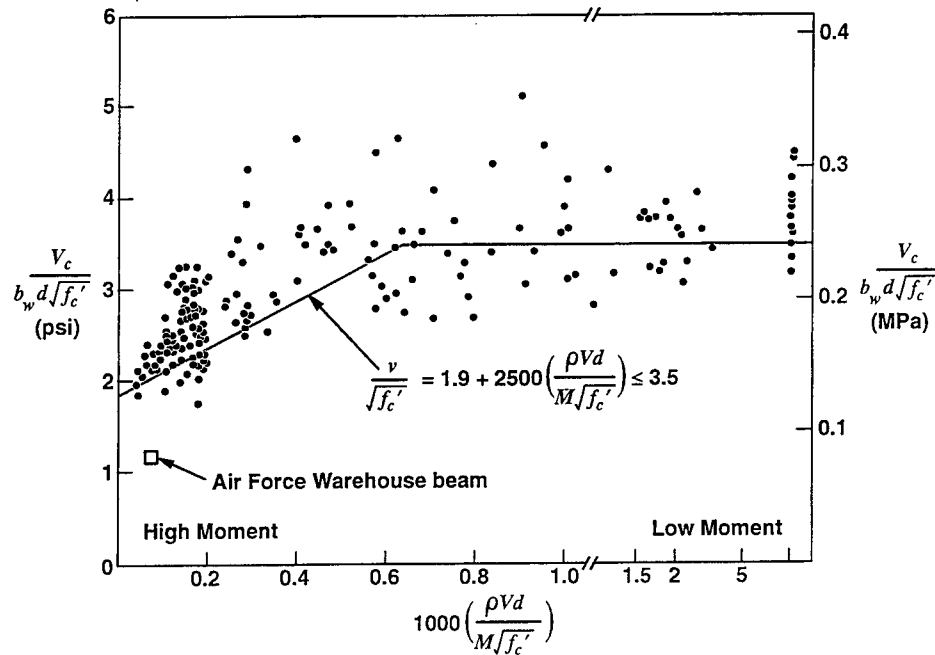


Figure 1.2 Derivation of ACI Expression for Diagonal Cracking Shear V_c
(Adapted from Ref. [4])

The 1962 ACI-ASCE Committee 326 recommendations[4] for changes to the ACI shear design provisions were initiated because of the August 1955 collapse[5]

of the Wilkins Air Force Depot warehouse in Shelby, Ohio and the 1956 collapse of a similar warehouse in Georgia. These collapses were caused by the failure of 915 mm deep beams which, at the failure locations, did not contain stirrups, and only had 0.45% of longitudinal reinforcement. The beams failed at a shear stress of only about 0.5 MPa, whereas the ACI Building Code[6], used in the design, permitted an allowable working stress of 0.6 MPa for the 20 MPa concrete used. At this time, the sensitivity of the failure shear stress, of this type of member, to size was not recognized and so, in investigating the failures at the Portland Cement Association (PCA) the research engineers chose to use one-third scale models. The PCA experiments[7] indicated that the 305 mm deep beams failed at a shear stress of about 1 MPa; that is, about twice the failure shear stress of the prototype. When an axial tensile stress of about 1.4 MPa was applied to a model beam the shear stress at failure was reduced by about 50%. The PCA engineers concluded that the presence of tensile stresses, in the prototype beams, caused by the restraint of shrinkage and thermal movements was the reason why the beams had failed at such low shear stresses. It so happens that the beams tested by Shioya et al., and shown in Fig. 1.1, had rather similar characteristics to the Air Force warehouse beams. The failure shear stress for the prototype warehouse beams and the PCA model beams without axial tension have also been plotted in Fig. 1.1. From this figure it seems clear that the 50% reduction in failure shear stress between the model and the prototype for the Air Force beams was primarily due to the size effect in shear, rather than the influence of axial tensile stresses.

Reinforced concrete members that contain ties or stirrups will not exhibit the same sensitivity to member size as the beams shown in Fig. 1.1. Members subjected to axial compression, members with more longitudinal reinforcement, and members with short shear spans will also be less sensitive to the size effect in shear. Thus, in many practical situations the size effect in shear will be negligibly small, while in other practical situations such as those shown in Fig. 1.1, the size effect will be very substantial. In this paper some analytical and some experimental studies will be reviewed with the objective of identifying more precisely those situations in which the size effect in shear is significant. As the analytical studies

will use the modified compression field theory[8] a discussion of the theory will be given.

2. MODIFIED COMPRESSION FIELD THEORY

The modified compression field theory was developed by observing the load-deformation response of a large number of reinforced concrete membrane element loaded in pure shear in the University of Toronto's membrane element tester[9,10] and shell element tester[11]. Figure 2.1 compares the calculated and observed response for one of these elements, which was called SE6[11]. The problem addressed by the modified compression field theory is to predict the relationship between the shear stress applied to such an element and the resulting shear strain.

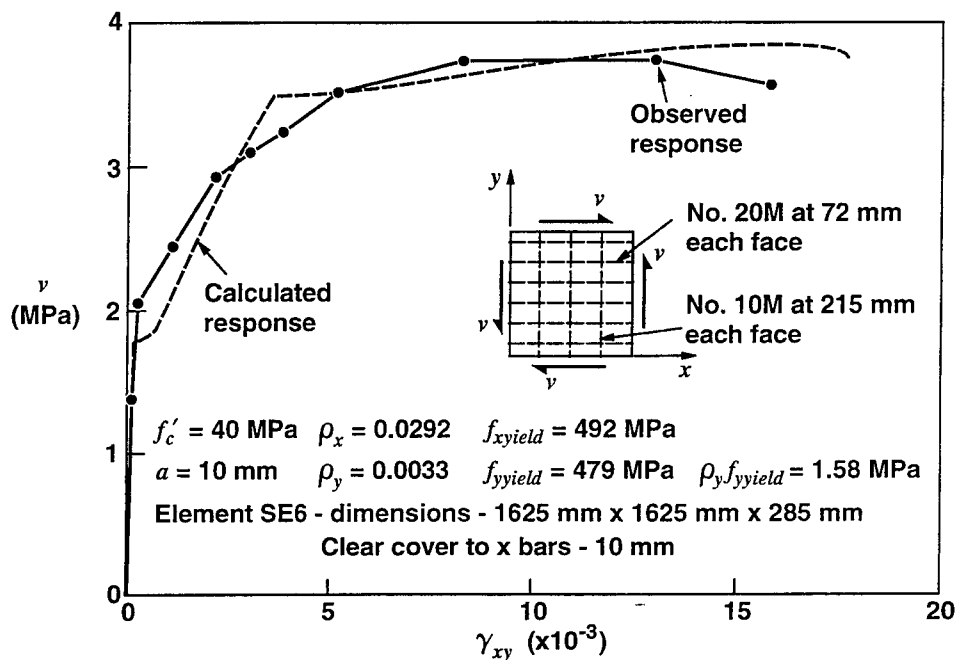


Figure 2.1 Comparison of Calculated and Observed Shear Response of Membrane Element SE6

Cracked reinforced concrete transmits shear in a relatively complex manner involving opening and closing of pre-existing cracks, formation of new cracks, interface shear transfer at rough crack surfaces, significant tensile stresses in the cracked concrete, and great variation of local stresses in both the concrete and reinforcement from point to point in the cracked concrete, with the highest

reinforcement stresses and the lowest concrete tensile stresses occurring at crack locations. The modified compression field theory attempts to capture the essential features of this behaviour without considering all of the details. In lieu of following the complex stress variations in the cracked concrete, only the average values of the stresses (that is, stresses averaged over a length greater than the crack spacing) and the stresses at the crack locations are considered.

Figure 2.2 summarizes the equilibrium, compatibility and stress-strain relationships used by the modified compression field theory. In these relationships θ is the angle between the x axis and the direction of the principal compressive average strain. Note that these average strains are measured over base lengths that are greater than the crack spacing. The basic simplifying assumption of both the compression field theory[12] and the modified compression field theory[8] is that "the direction that is subjected to the largest average compressive stress will coincide with the direction that is subjected to the largest average compressive strain." For specified applied loads, the angle θ , the average stresses and the average strains can be determined by solving the given equilibrium equations in terms of average stresses, the given compatibility equations in terms of average strains and the given average stress-average strain relationships.

The maximum shear stress that the element can resist may be governed not by the average stresses, but rather, by the local stresses at the crack locations. In checking the conditions at a crack, the actual complex crack pattern is idealized as a series of parallel cracks, all occurring at angle θ and spaced at a distance s_θ apart. It is assumed that for crack widths greater than about 0.05 mm no significant tensile stresses can be transmitted normal to the crack. However, shear stresses, v_{ci} , can be transmitted across the crack. The maximum possible value of v_{ci} is assumed to be related to the crack width, w , and the maximum aggregate size, a .

Solving all the equations given in Fig. 2.2 is of course very tedious if performed by hand but is quite straightforward with a programmable calculator or other small computer. A short (about 300 lines of BASIC) program called MEMBRANE, which performs these calculations is given in the textbook *Prestressed Concrete Structures*[12]. Program RESPONSE, which is also given in

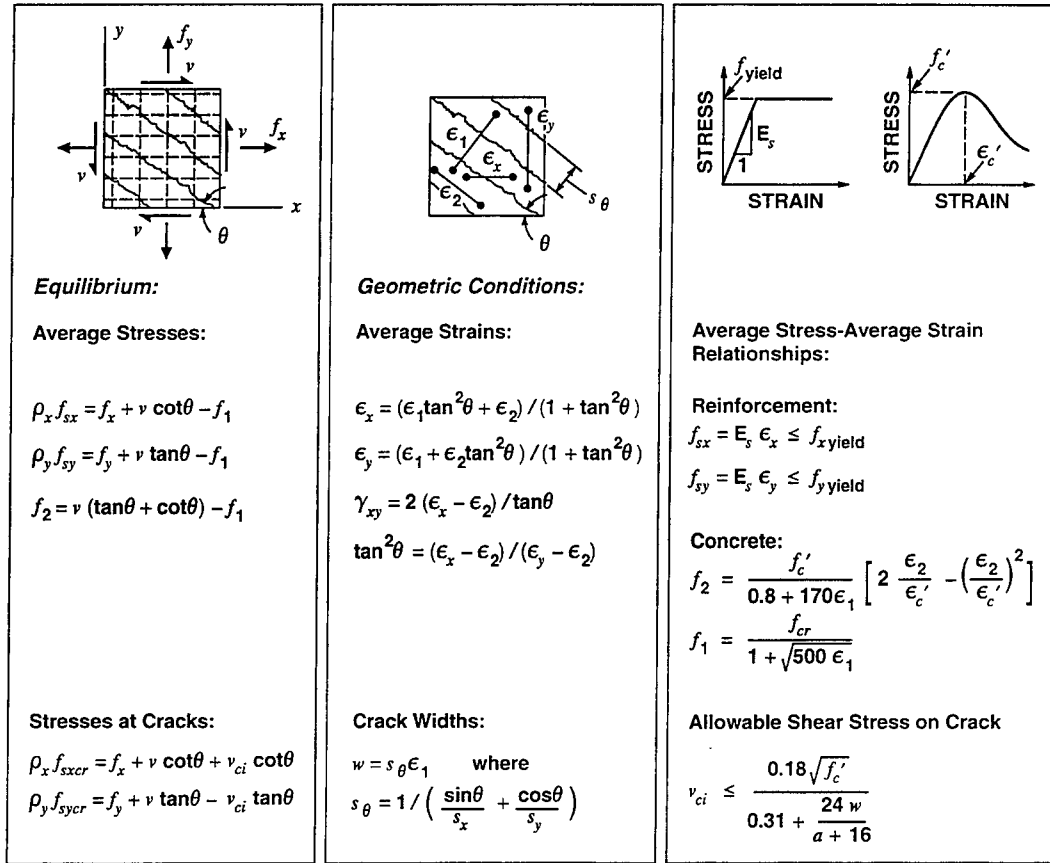


Figure 2.2 A Summary of the Relationships Used in the Modified Compression Field Theory

this textbook, is somewhat more convenient to use than program MEMBRANE and can be used to solve for membrane elements provided that there is no applied axial stress in the y direction. The results obtained from program RESPONSE for element SE6 are summarized in Table 2.1 and are plotted in Fig. 2.1.

The modified compression field theory[8] differs from the earlier compression field theory[12] in that it accounts for the presence of tensile stresses in the cracked concrete. Using the second equilibrium equation from Fig. 2.2, the shear applied to the element, v , can be related to the average stress in the weaker y reinforcement, f_{sy} , and the average tensile stress in the cracked concrete, f_1 , as

$$v = f_1 \cot \theta + \rho_y f_{sy} \cot \theta \quad (2.1)$$

Table 2.1 Predicted Response of Membrane Element SE6
(Crack spacing parameters: $s_x = 195$ mm; $s_y = 450$ mm).

Average Strains ($\times 10^{-3}$)					Average Stresses (MPa)					Stress at Crack (MPa)				w (mm)	v (MPa)	Comments
ϵ_1	ϵ_x	ϵ_y	γ_{xy}	θ	f_{xx}	f_{yy}	f_1	f_2	f_{2max}	f_{sxc}	f_{syc}	v_{ci}	v_{cmax}			
0.088	-0.01	0	0.19	42.9°	-3	0	2.06	2.39	40.0	-	-	-	-	0	1.78	uncracked
0.50	0.14	0.25	0.59	39.8°	29	51	1.39	2.40	40.0	77	472	0	2.81	0.10	1.87	$f_{syc} \approx f_{yyield}$
1.00	0.27	0.59	1.09	37.0°	55	118	1.22	3.22	40.0	99	479	0.06	2.27	0.21	2.13	
1.50	0.39	0.94	1.57	35.5°	78	187	1.12	4.02	39.8	128	479	0.24	1.89	0.31	2.44	
2.50	0.60	1.63	2.57	34.1°	120	326	0.99	5.55	35.1	189	479	0.72	1.42	0.53	3.04	
3.50	0.79	2.34	3.55	33.2°	157	467	0.78	6.90	31.4	243	479	1.13	1.13	0.75	3.52	$v_{ci} = v_{cmax}$
6.00	1.01	4.44	5.58	29.2°	202	479	0.41	7.88	24.8	261	479	0.73	0.73	1.35	3.53	
9.00	1.19	7.04	7.83	26.6°	239	479	0.25	8.79	19.8	281	479	0.50	0.50	2.10	3.62	
20.00	1.52	16.5	16.3	23.3°	304	479	0.10	10.6	11.4	326	479	0.23	0.23	4.92	3.87	$v = v_{max}$
21.50	1.52	17.8	17.2	23.3°	304	479	0.09	10.5	10.7	324	479	0.22	0.22	5.29	3.85	$f_2 \approx f_{2max}$

The above two components of the shear resistance can be thought of as a concrete contribution, v_c , plus a steel contribution, v_s . The mechanisms involved in transmitting the average tensile stresses, f_1 , through the cracked concrete are sensitive to the width of the cracks. For two geometrically similar reinforced concrete elements, with one element being twice the size of the other, the crack widths, for given strains, will be about twice as large for the larger element. Because of this, the average tensile stress that can be transmitted in the larger element will typically be smaller, and hence, the shear stress at failure will be smaller.

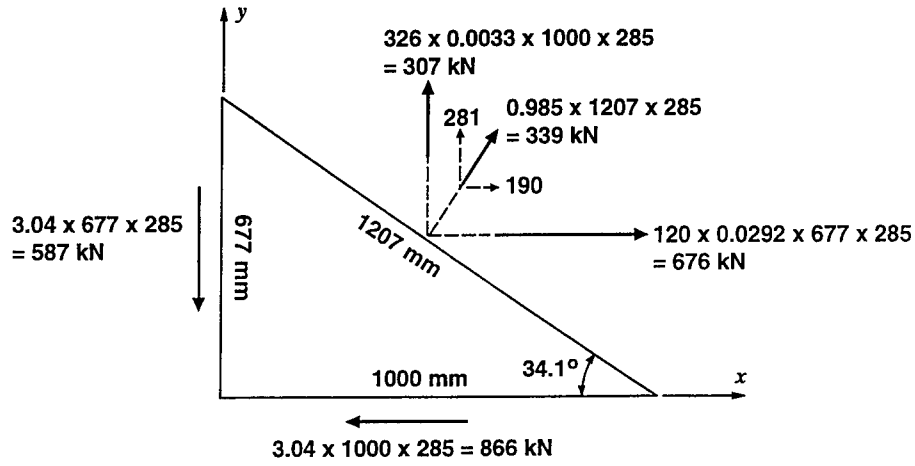
Because the size effect in shear is related to the mechanisms involved in transmitting f_1 through cracked concrete it is appropriate to discuss these mechanisms in more detail. Figure 2.3 shows two free body diagrams of a corner portion of element SE6 where the corner has been cut off at an angle of 34.1°. This is the calculated direction of principal compressive average strain when the principal tensile average strain, ϵ_1 , equals 2.5×10^{-3} . See Table 2.1. At this strain, the shear stress applied to the element is predicted to be 3.04 MPa. Figure 2.3(a) illustrates how this applied shear stress is balanced by the average reinforcement stresses and the average tensile stress in the concrete, f_1 , which at this stage can be calculated as

$$\begin{aligned}
 f_1 &= \frac{f_{cr}}{1 + \sqrt{500\epsilon_1}} \\
 &= \frac{0.33\sqrt{40}}{1 + \sqrt{500 \times 0.0025}} = 0.985 \text{ MPa}
 \end{aligned}
 \tag{2.2}$$

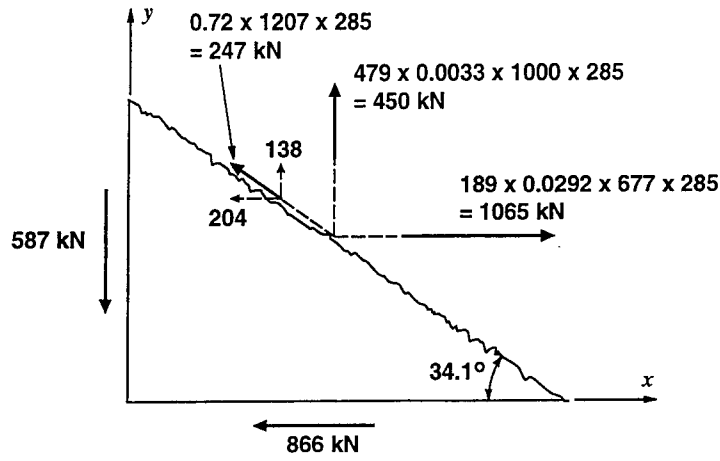
Note that the vertical force transmitted across the diagonal plane by the vertical component of the force resulting from the average tensile stress in the concrete is 281 kN, while the vertical force transmitted by the average tensile stresses in the y reinforcement is 307 kN. In terms of Eq. (2.1) these two components are equivalent to

$$\begin{aligned}
 v &= f_1 \cot\theta + \rho_y f_{sy} \cot\theta \\
 &= 0.985 \cot 34.1 + 0.0033 \times 326 \cot 34.1 \\
 &= 1.455 + 1.589 = 3.04 \text{ MPa}
 \end{aligned}$$

Figure 2.3(b) examines the stresses required to be transmitted across a crack that has formed at 34.1° to the x axis. Cracks in an element such as SE6 form in a number of different directions. See Fig. 2.4. The initial cracks formed at about 45° to the x reinforcement. As the shear stress was increased cracks formed at about 35° , 28° and 20° to the stronger x reinforcement. With an increase in shear stress the width of the earlier cracks remained relatively constant while the width of the most recently formed cracks increased. At a particular load level, the modified compression field theory checks the stresses for a crack direction that corresponds to the current calculated value of θ . For element SE6 this angle decreases from 42.9° to 23.3° as the shear stress increases from 1.78 MPa to 3.87 MPa. See Table 2.1. For an angle of 34.1° the maximum vertical force that the y reinforcement can transmit across the diagonal crack is 450 kN. As this force is not large enough to balance the applied vertical force of 587 kN, a shear force of 247 kN is required to be transmitted across the crack surface, which is equivalent to a shear stress of 0.72 MPa.



(a) Equilibrium in Terms of Average Stresses



(b) Equilibrium in Terms of Stresses at Crack

Figure 2.3 Equilibrium of Element SE6 When $\epsilon_1 = 2.5 \times 10^{-3}$ and $\nu = 3.04$ MPa

The maximum shear stress that can be transmitted across a crack that has no compressive stress applied to it is assumed to be

$$v_{cimax} = \frac{0.18\sqrt{f'_c}}{0.31 + \frac{24w}{a + 16}} \quad (2.3)$$

where the crack width, w , is taken as

$$w = s_\theta \epsilon_1 \quad (2.4)$$

and the crack spacing s_θ is taken as

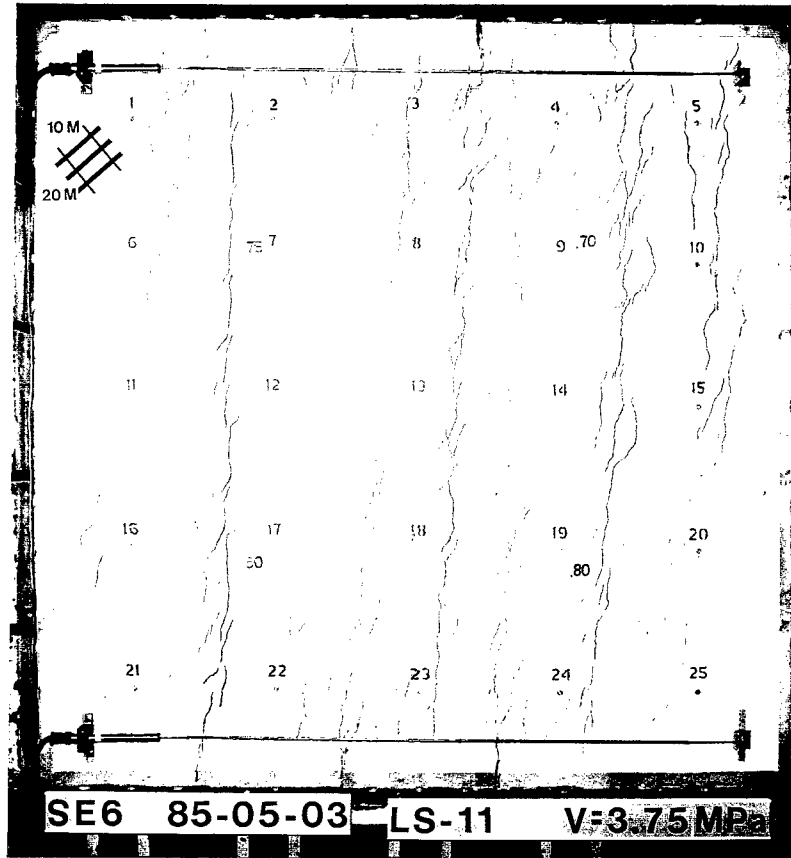


Figure 2.4 Observed Crack Patterns for Element SE6

$$s_{\theta} = \frac{1}{\frac{\sin\theta}{s_x} + \frac{\cos\theta}{s_y}} \quad (2.5)$$

The crack spacing when the cracks are perpendicular to the x reinforcement, s_x may be taken as

$$s_x = s_{\max x} + 0.1 d_{bx} / \rho_x \quad (2.6)$$

where $s_{\max x}$ is the maximum distance that the concrete in the shear area is away from a bar in the x direction and d_{bx} is the bar diameter of the x reinforcement. Similarly the crack spacing when the cracks are perpendicular to the y reinforcement may be taken as

$$s_y = s_{\max y} + 0.1 d_{by} / \rho_y \quad (2.7)$$

The calculation of s_x and s_y for element SE6 is illustrated in Fig. 2.5 where it can be seen that s_x equals 195 mm and s_y equals 450 mm. Hence,

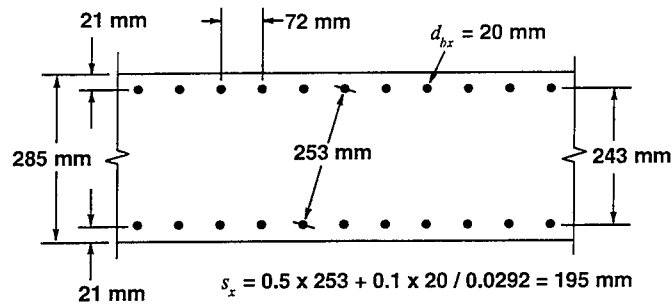
$$s_\theta = 1/(\sin 34.1/195 + \cos 34.1/450) = 212 \text{ mm}$$

$$w = 212 \times 2.5 \times 10^{-3} = 0.53 \text{ mm}$$

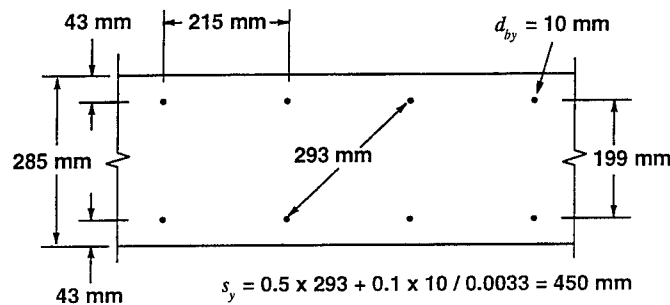
and

$$v_{cmax} = \frac{0.18\sqrt{40}}{0.31 + \frac{24 \times 0.53}{10 + 16}} = 1.42 \text{ MPa}$$

As this maximum shear stress which can be transmitted is considerably greater than the 0.72 MPa shear stress required to transmit the f_1 given in Eq. (2.2), no reduction in this value of f_1 is required.



(a) Calculation of crack spacing s_x



(b) Calculation of crack spacing s_y

Figure 2.5 Calculation of Crack Spacing Parameters s_x and s_y for Element SE6

It can be seen from Table 2.1 that for values of ϵ_1 greater than 3×10^{-3} the shear stress on the crack is controlled by v_{cimax} . The influence of this "crack slip" on the resulting value of f_1 that can be transmitted through the cracked concrete is illustrated in Fig. 2.6. When the shear on the crack reaches its limiting value, the average tension in the cracked concrete is limited to

$$f_1 = v_{cimax} \tan \theta \quad (2.8)$$

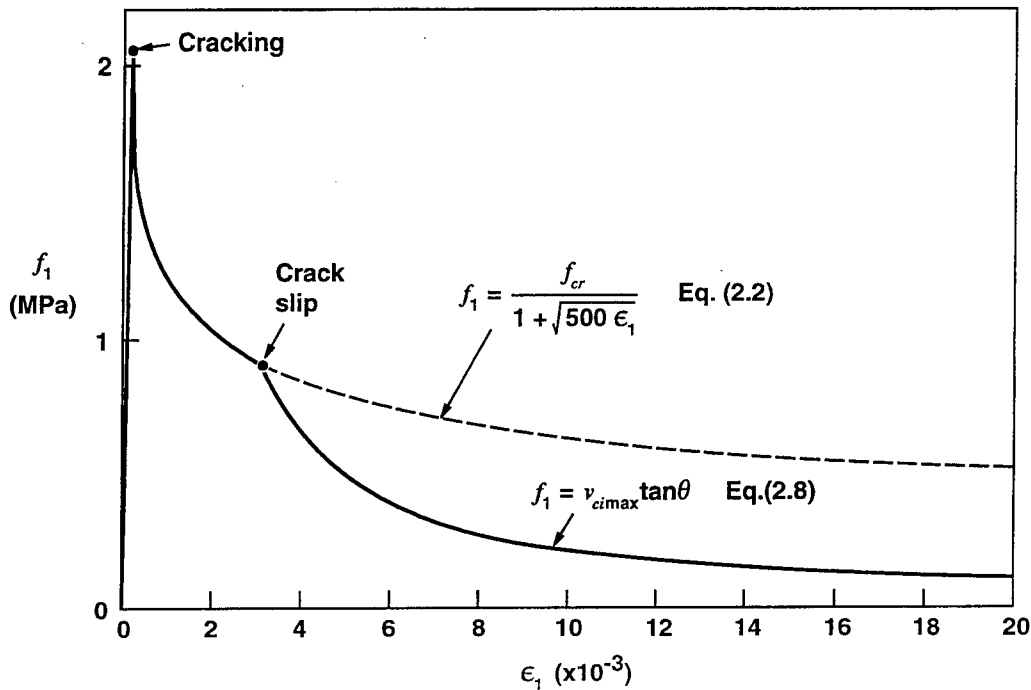


Figure 2.6 Calculated Values of f_1 for Element SE6

If the value of f_1 is governed by Eq. (2.8) rather than Eq. (2.2), the size of the member will influence the failure shear. This point is illustrated in Fig. 2.7, which plots the predicted failure shear stresses for two series of elements. One series is geometrically similar to SE6 and is loaded in pure shear. The two smallest elements of this series (s_x equals 12 mm and 24 mm) are not governed by crack slip and hence, are predicted to fail at the same shear stress (4.53 MPa). The three largest elements all have such low values of f_1 that the predicted failure shears are nearly equal to 3.71 MPa, which is the value obtained by assuming zero tension in

the cracked concrete. It can be concluded that this type of element, which contains about 3 times the minimum amount of "stirrups" given by the AASHTO-LRFD specifications[14], is not very sensitive to the size effect in shear.

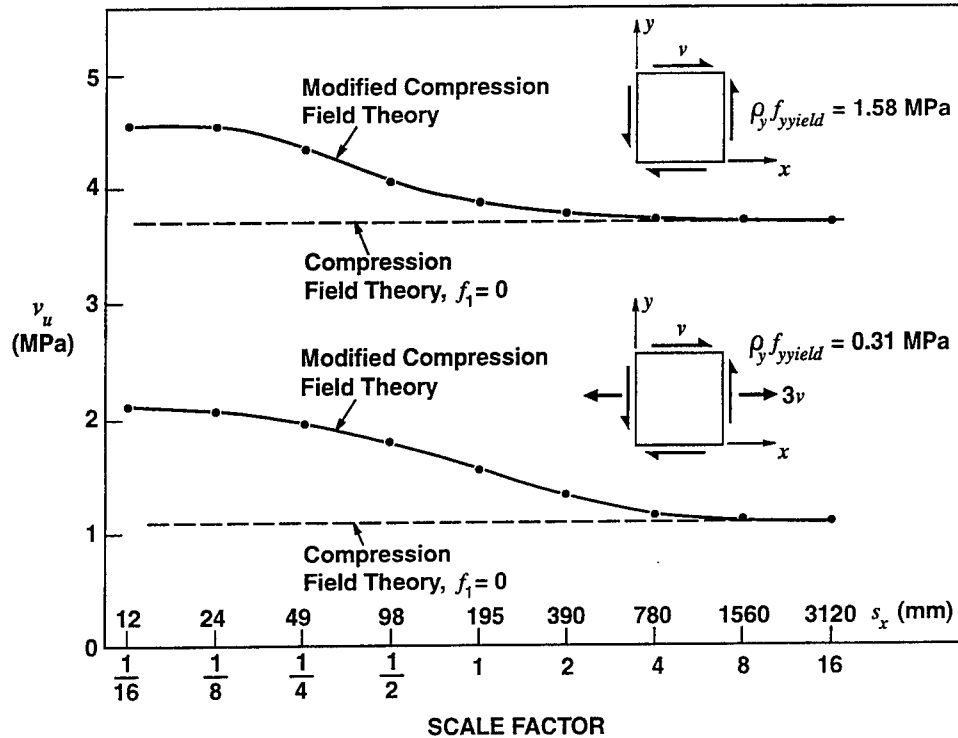


Figure 2.7 Influence of Element Size on Predicted Failure Shear Stress of Two Series of Elements Similar to SE6

The second series of elements plotted in Fig. 2.7 contain only about one-fifth as much transverse reinforcement as element SE6 ($\rho_y = 0.00064$) and are subjected to combined tension and shear with the ratio of axial tensile stress to shear stress being set at 3. Once again, crack slip is not critical for the two smallest elements and hence, both are predicted to fail at about the same shear stress (2.10 MPa). The three largest elements have very low values of f_1 and hence, their predicted failure shears are close to 1.16 MPa, which is the value obtained by assuming zero tension in the cracked concrete. Note that this second series of elements displays a larger size effect than the first series. The failure shear stress of the largest element in the second series is only 55% of the failure shear stress of the smallest element. For the first series this ratio of failure shear stress of the largest element to failure shear stress of the smallest element is 82%.

Of the two components, v_c and v_s , of the shear resistance expressed in Eq. (2.1), the size effect influences only the v_c component. Hence, as the amount of "stirrups", ρ_y , increases, the importance of the size effect diminishes. This point is illustrated in Fig. 2.8, which compares the predicted shear stresses at failure for the two series of elements. In one series the crack spacing is taken as 300 mm, while in the other it is taken as 2000 mm. It is assumed that the amount of longitudinal (x) reinforcement and the axial loading of the elements is such that the longitudinal strain ϵ_x , is held constant at 0.5×10^{-3} . It can be seen that the predicted shear stress at failure becomes more sensitive to crack spacing, and hence, member size as the amount of stirrup reinforcement, ρ_y , is reduced. When ρ_y is zero, the element with the 2000 mm crack spacing is predicted to fail at only about half the shear stress of the element with the 300 mm crack spacing. The minimum stirrup amount shown in the figure is that given by the AASHTO-LRFD specifications, namely

$$(\rho_y f_{yield})_{\min} = 0.083 \sqrt{f'_c} \quad (2.9)$$

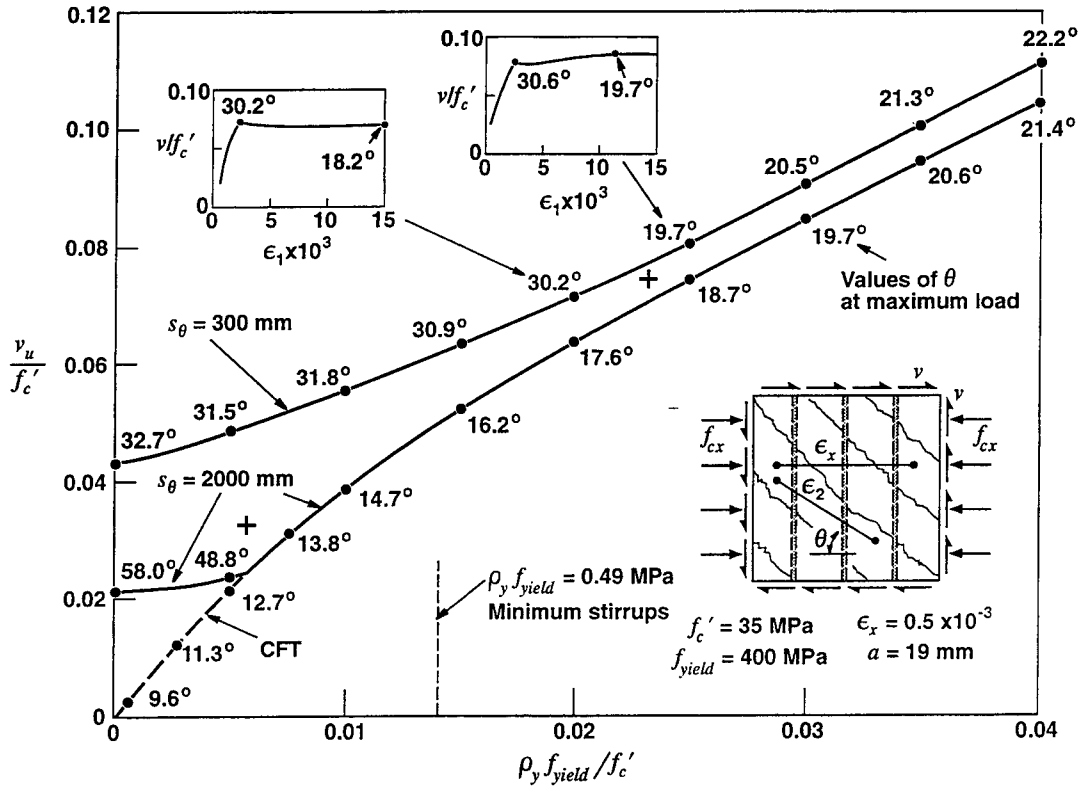


Figure 2.8 Influence of Crack Spacing on the Predicted Shear Strengths of a Series of Elements with Different Amounts of Stirrups

3. THE BETA METHOD FOR PREDICTING SHEAR STRENGTH

While the equations of the modified compression field theory, given in Fig. 2.2, can be easily solved with the aid of a small computer program, they are not suitable for hand calculations. If the primary objective is to obtain an estimate of the maximum shear stress, v_{\max} , that an element can resist, then the equations can be re-arranged into a form suitable for hand design. The resulting procedure[15] can be referred to as the beta method. This method forms the basis of the shear design procedures of the AASHTO-LRFD specifications[14] and is included in the Canadian concrete code[16].

It is assumed that the y direction reinforcement is the weaker reinforcement and that this reinforcement is yielding when the maximum shear stress is reached. Equation (2.1) can then be expressed as

$$v_{\max} = \beta \sqrt{f'_c} + \rho_y f_{\text{yield}} \cot \theta \quad (3.1)$$

The values of β and θ are taken from Table 3.1 for elements that contain more than the minimum amount of y reinforcement given by Eq. (2.9). For such elements the size effect in shear is neglected. For elements with less than the minimum amount of transverse reinforcement, the values of β and θ are taken from Table 3.2. In these cases the size effect in shear is accounted for by the crack spacing parameter s_x . The values in Table 3.2 were derived assuming that the maximum aggregate size was 19 mm. However, the tabulated values can be used for other aggregate sizes by using an equivalent spacing parameter, s_{xe} , where

$$s_{xe} = \frac{35}{a + 16} s_x \quad (3.2)$$

Table 3.1 Values of β and θ for Members Containing at Least the Minimum Amount of Stirrups

$\frac{v}{f'_c}$		Longitudinal Strain $\epsilon_x \times 1000$						
		≤ 0	≤ 0.25	≤ 0.5	≤ 0.75	≤ 1.0	≤ 1.5	≤ 2.0
≤ 0.05	θ	27.0°	28.5°	29.0°	33.0°	36.0°	41.0°	43.0°
	β	0.405	0.290	0.208	0.197	0.185	0.162	0.143
≤ 0.075	θ	27.0°	27.5°	30.0°	33.5°	36.0°	40.0°	42.0°
	β	0.405	0.250	0.205	0.194	0.179	0.158	0.137
≤ 0.1	θ	23.5°	26.5°	30.5°	34.0°	36.0°	38.0°	39.0°
	β	0.271	0.211	0.200	0.189	0.174	0.143	0.120
≤ 0.125	θ	23.5°	28.0°	31.5°	34.0°	36.0°	37.0°	38.0°
	β	0.216	0.208	0.197	0.181	0.167	0.133	0.112
≤ 0.15	θ	25.0°	29.0°	32.0°	34.0°	36.0°	36.5°	37.0°
	β	0.212	0.203	0.189	0.171	0.160	0.125	0.103
≤ 0.2	θ	27.5°	31.0°	33.0°	34.0°	34.5°	35.0°	36.0°
	β	0.203	0.194	0.174	0.151	0.131	0.100	0.083
≤ 0.25	θ	30.0°	32.0°	33.0°	34.0°	35.5°	38.5°	41.5°
	β	0.191	0.167	0.136	0.126	0.116	0.108	0.104

Table 3.2 Values of β and θ for Members Containing Less than the Minimum Amount of Stirrups

s_x (mm)		Longitudinal Strain $\epsilon_x \times 1000$					
		≤ 0	≤ 0.25	≤ 0.50	≤ 1.00	≤ 1.50	≤ 2.00
≤ 125	θ	27°	29°	32°	34°	36°	38°
	β	0.406	0.309	0.263	0.214	0.183	0.161
≤ 250	θ	30°	34°	37°	41°	43°	45°
	β	0.384	0.283	0.235	0.183	0.156	0.138
≤ 500	θ	34°	39°	43°	48°	51°	54°
	β	0.359	0.248	0.201	0.153	0.127	0.108
≤ 1000	θ	37°	45°	51°	56°	60°	63°
	β	0.335	0.212	0.163	0.118	0.095	0.080
≤ 2000	θ	41°	53°	59°	66°	69°	72°
	β	0.306	0.171	0.126	0.084	0.064	0.052

As an example of using the beta method assume we wish to have a shear capacity of 2.625 MPa for an element made from 35 MPa concrete, and that the axial strain, ϵ_x , is 0.5×10^{-3} . As v_{\max}/f'_c is 0.075, the values of β and θ from Table 3.1 are 0.205 and 30° . Thus Eq. (3.1) becomes

$$2.625 = 0.205\sqrt{35} + \rho_y f_{\text{yield}} \cot 30^\circ$$

Hence, the amount of transverse reinforcement required is

$$\rho_y f_{\text{yield}} = 0.815 \text{ MPa}$$

As this is greater than the minimum value of 0.491 MPa required by Eq. (2.9) we were correct to use Table 3.1 rather than Table 3.2 to determine β and θ . The point representing a value of v_{\max}/f'_c of 0.075 at a value of $\rho_y f_{\text{yield}}/f'_c$ of 0.0233 is shown as a small cross on Fig. 2.8.

As a second example we will determine the shear capacity of an element with a very small amount of transverse reinforcement such that $\rho_y f_{\text{yield}}$ equals 0.20 MPa. We will assume that the size of the element is such that s_x is 1000 mm, with a maximum aggregate size of 19 mm, and that ϵ_x again equals 0.5×10^{-3} . From Table 3.2 the values of β and θ are 0.163 and 51° . Hence,

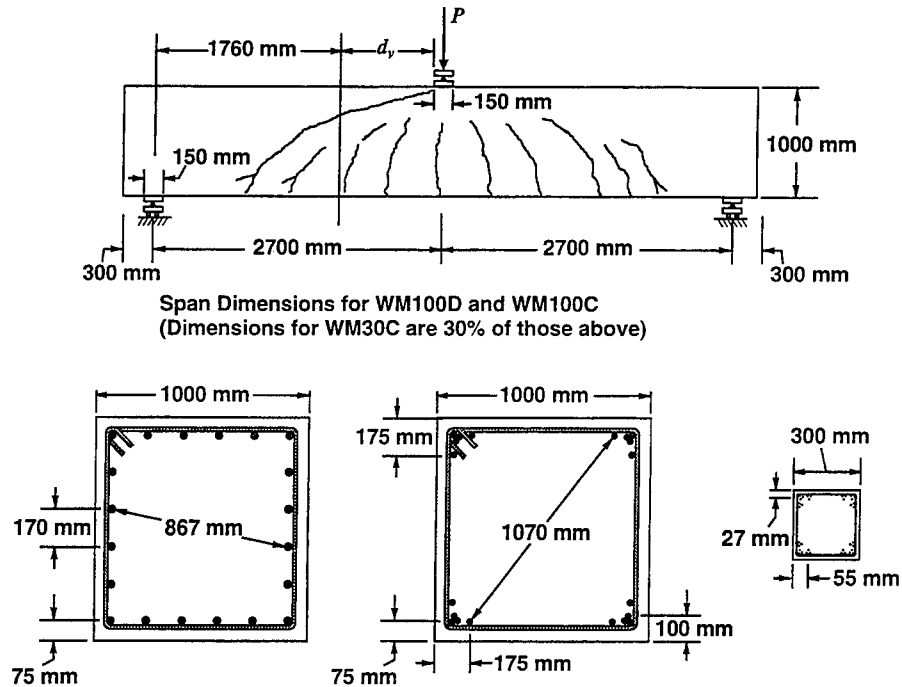
$$\begin{aligned} v_{\max} &= 0.163\sqrt{35} + 0.20 \cot 51^\circ \\ &= 0.964 + 0.162 = 1.126 \text{ MPa} \\ &= 0.032 f'_c \end{aligned}$$

The point corresponding to a value of v_{\max}/f'_c of 0.0322 at a value of $\rho_y f_{\text{yield}}/f'_c$ of 0.0057 is shown as a small cross on Fig. 2.8. It can be seen that this point lies between the values predicted by the modified compression field theory for s_θ equals 300 mm and s_θ equals 2000 mm.

4. "COLUMN" TESTS AT THE UNIVERSITY OF TORONTO

As part of collaborative research between the structural engineering groups at the University of California, San Diego, and the University of Toronto, three reinforced concrete specimens were tested at the University of Toronto in the spring of 1997. These experiments were designed to investigate the possible magnitude of the size effect in shear for square reinforced columns. The specimens contained 1.4% of longitudinal reinforcement and a small amount of transverse reinforcement such that $\rho_y f_{y\text{yield}}$ equalled 0.192 MPa. Two of the specimens had cross-sectional dimensions of 1 m \times 1 m, while the third was 0.3 m \times 0.3 m. The specimens were loaded in single curvature such that the ratio of shear span to overall depth was 2.7. No axial load was applied. Further details of the test program are given in Fig. 4.1. Note that specimen WM100D contained 20 longitudinal bars uniformly distributed around the perimeter, while WM100C had its 20 longitudinal bars concentrated near the corners. Specimen WM30C was a 30% model of WM100C.

The specimens were loaded as simply supported beams with a point load at mid-span. See Fig. 4.1. At a number of stages during each load test the displacement was held about constant while the cracks were marked with a felt pen and the widths of the cracks were measured with a crack comparator (accurate to 0.05 mm). Figure 4.2 shows the observed crack patterns and the measured crack widths for 6 stages in the test of specimen WM100D. Thus, for example, Fig. 4.2(c) shows the appearance of the specimen just after the point load at the centre of the beam reached a value of 1572 kN and the mid-span displacement reached a value of 18.4 mm. This point load caused a shear force of 786 kN in the beam. The dead load of this 1 m by 1 m specimen was 24 kN per metre. Hence, at a section 1 m from the midspan, the total shear force applied to the section was 786 kN plus 24 kN, that is, 810 kN. If this shear force is divided by the total cross-sectional area we obtain an average shear stress value of 0.810 MPa. The test described in Fig. 4.1 is intended to simulate a column fixed at the base and loaded with a horizontal point load 2.7 m above the base. The horizontal displacement of this point load divided by the 2.7 m storey height is called the storey drift. For the stage shown in

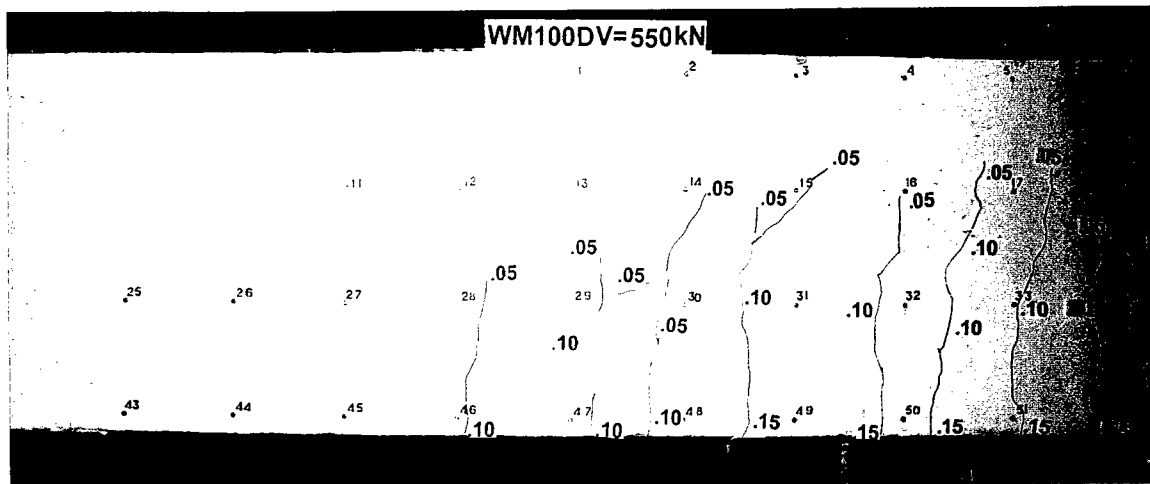


Specimen	WM100D	WM100C	WM30C
Concrete	$f'_c = 38 \text{ MPa}$ $a = 10 \text{ mm}$	$f'_c = 41 \text{ MPa}$ $a = 10 \text{ mm}$	$f'_c = 41 \text{ MPa}$ $a = 10 \text{ mm}$
Longitudinal Reinforcement	20-30 mm bars $f_{xyield} = 550 \text{ MPa}$ $\rho_x = 0.0140$	20-30 mm bars $f_{xyield} = 550 \text{ MPa}$ $\rho_x = 0.0140$	36-6.6 mm wires $f_{xyield} = 629 \text{ MPa}$ $\rho_x = 0.0137$
Transverse Reinforcement	9.5 mm bars at 375 mm $f_{yyield} = 508 \text{ MPa}$ $\rho_y f_{yyield} = 0.192 \text{ MPa}$	9.5 mm bars at 375 mm $f_{yyield} = 508 \text{ MPa}$ $\rho_y f_{yyield} = 0.192 \text{ MPa}$	2.64 mm wires at 98 mm $f_{yyield} = 520 \text{ MPa}$ $\rho_y f_{yyield} = 0.194 \text{ MPa}$

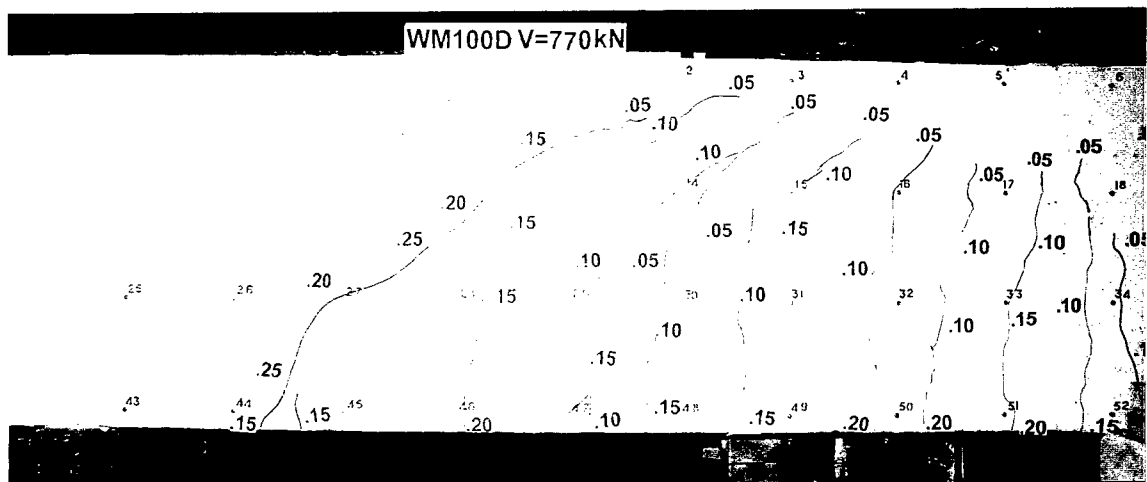
Figure 4.1 Details of Specimens Tested at the University of Toronto

Fig. 4.2(c) this storey drift is 0.68%. By comparing Fig. 4.2(b) and Fig. 4.2(c) it can be seen that as the shear stress was increased from 0.794 MPa to 0.810 MPa the width of the diagonal cracks increased from 0.25 mm to 4.5 mm indicating that a shear failure was imminent. The appearance of the specimen at the maximum load is shown in Fig. 4.2(d). By the time the storey drift reached 1.84% the average shear stress that the section could resist had reduced to 0.280 MPa, and many of the stirrups had fractured. See Fig. 4.2(f).

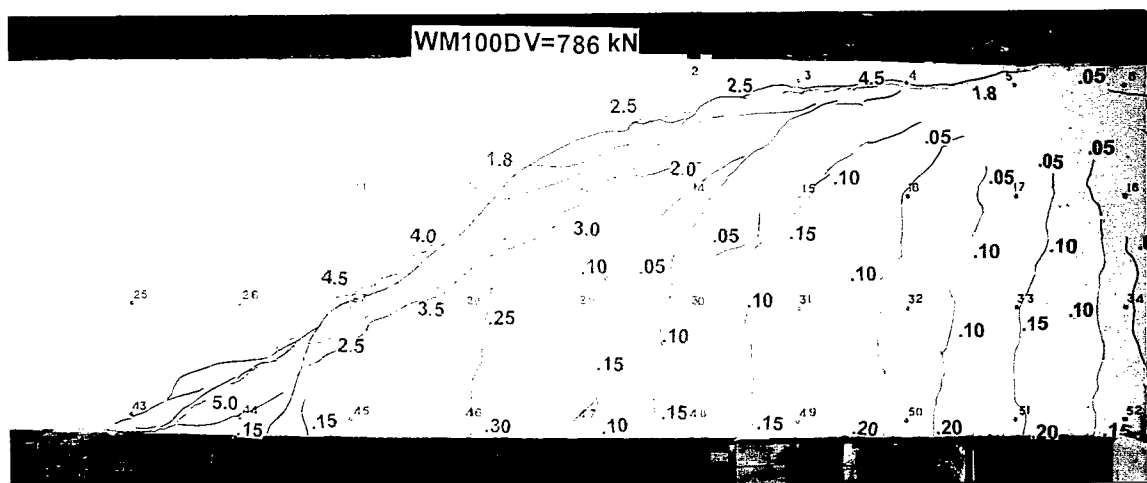
Figure 4.3 shows the observed crack patterns and the measured crack widths for 5 stages during the test of specimen WM100C. This specimen differed from



(a) Shear Stress = 0.574 MPa; Drift = 0.24%

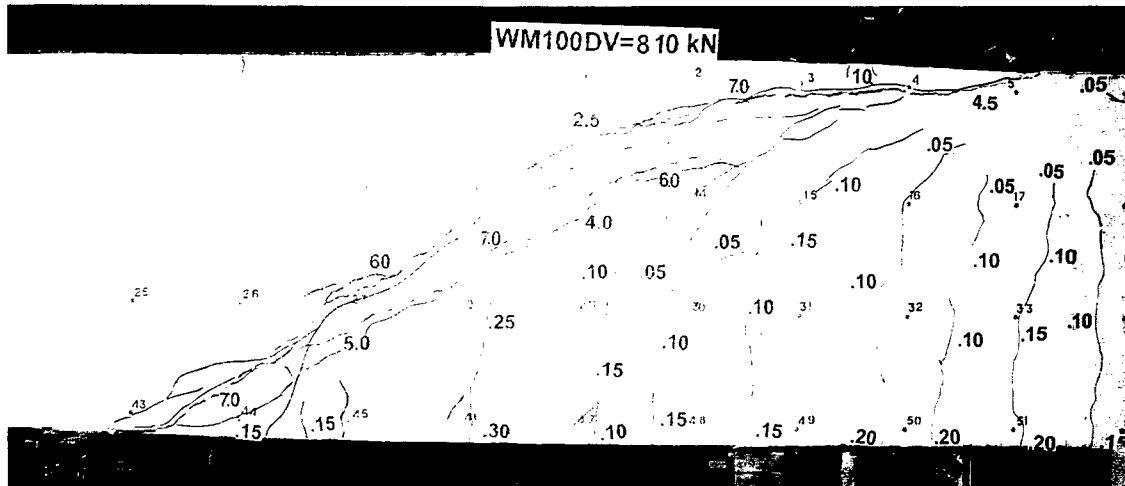


(b) Shear Stress = 0.794 MPa; Drift = 0.40%

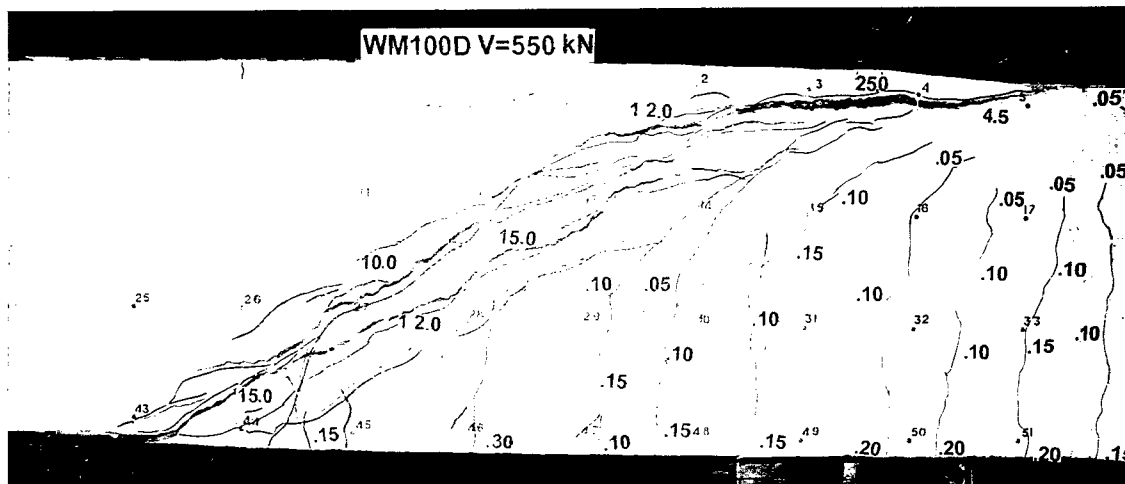


(c) Shear Stress = 0.810 MPa; Drift = 0.68%

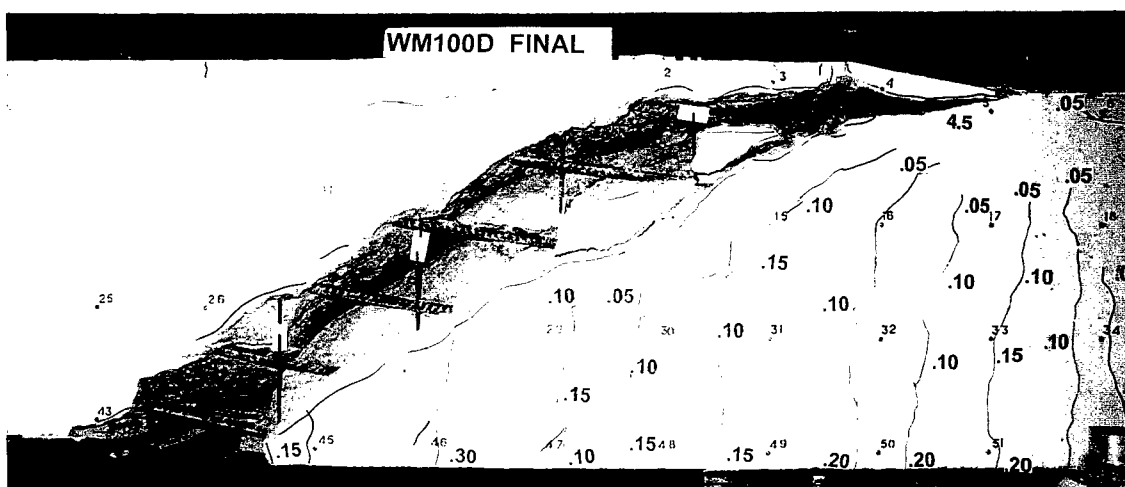
Figure 4.2 Crack Patterns and Measured Crack Widths (mm) for Specimen WM100D



(d) Shear Stress = 0.834 MPa; Drift = 0.75%

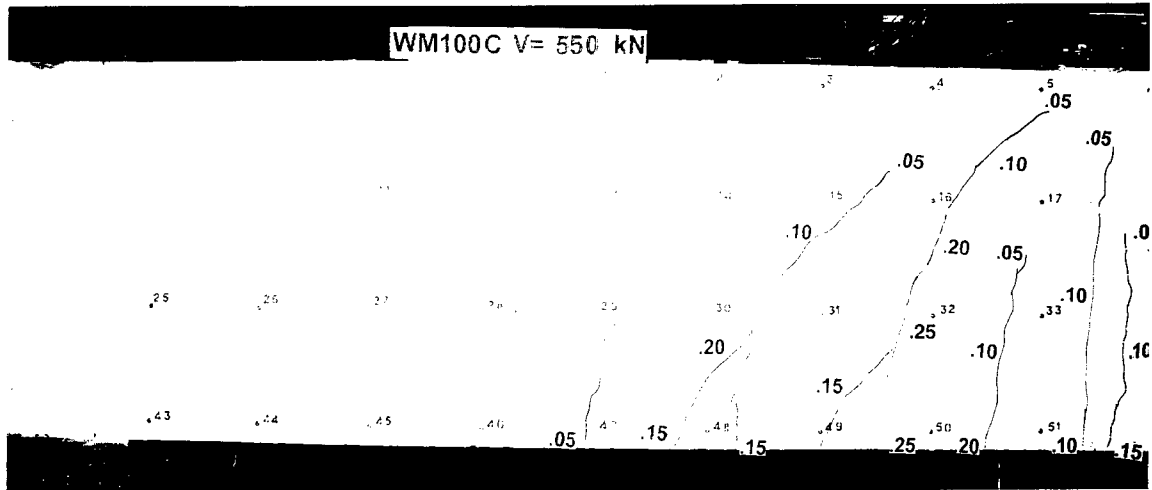


(e) Shear Stress = 0.574 MPa; Drift = 1.17%

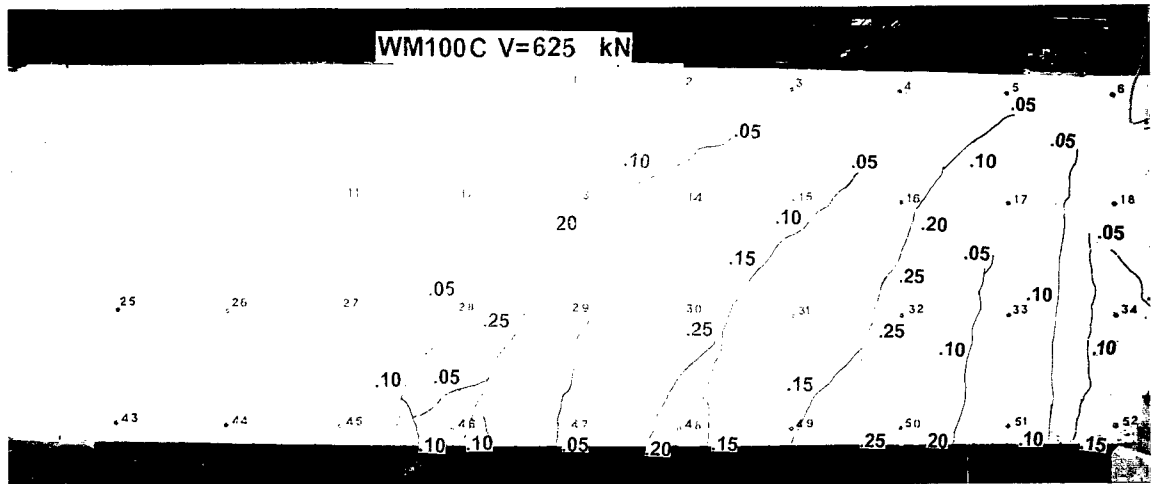


(f) Shear Stress = 0.280 MPa; Drift = 1.84%

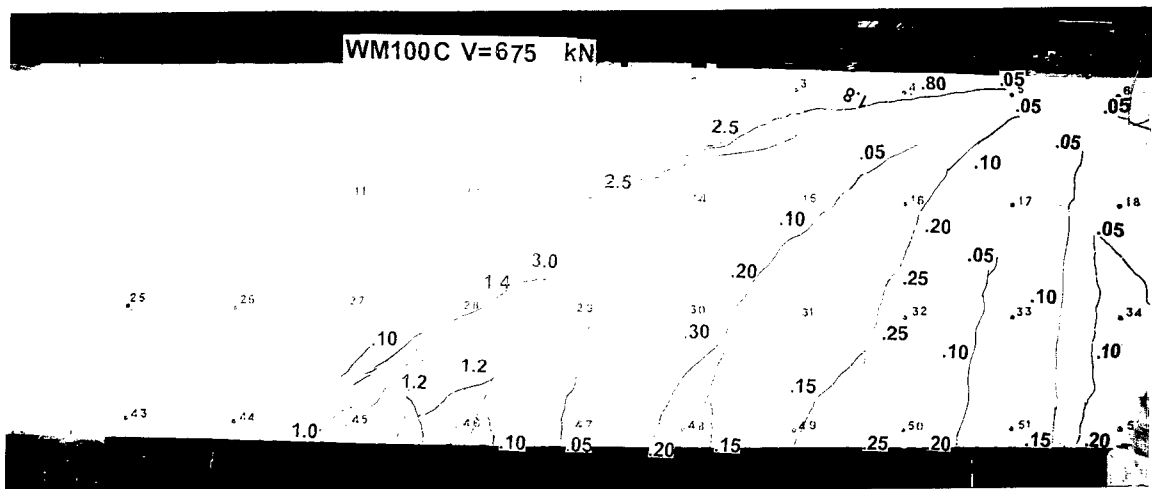
Figure 4.2 Crack Patterns and Measured Crack Widths (mm) for Specimen WM100D (continued)



(a) Shear Stress = 0.574 MPa; Drift = 0.24%

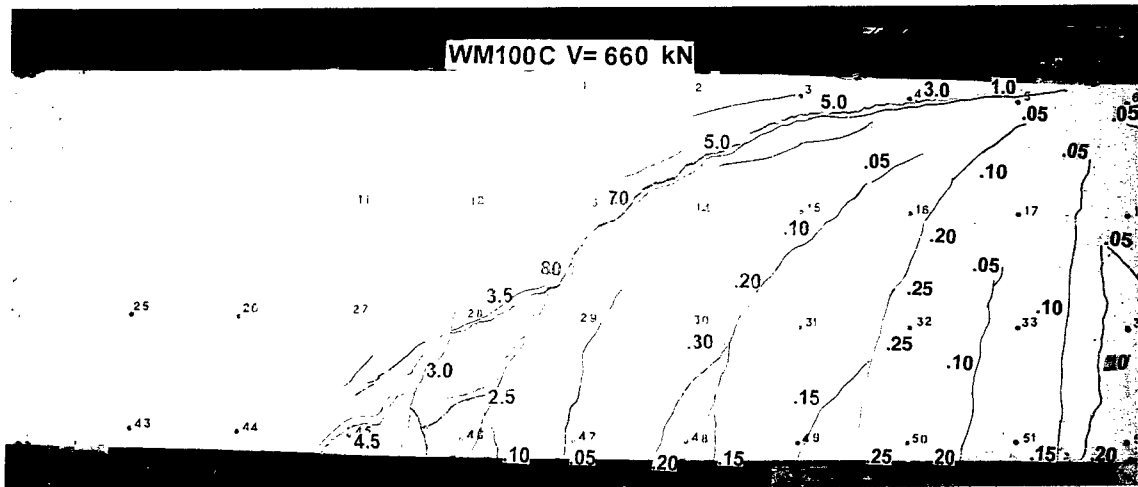


(b) Shear Stress = 0.649 MPa; Drift = 0.30%

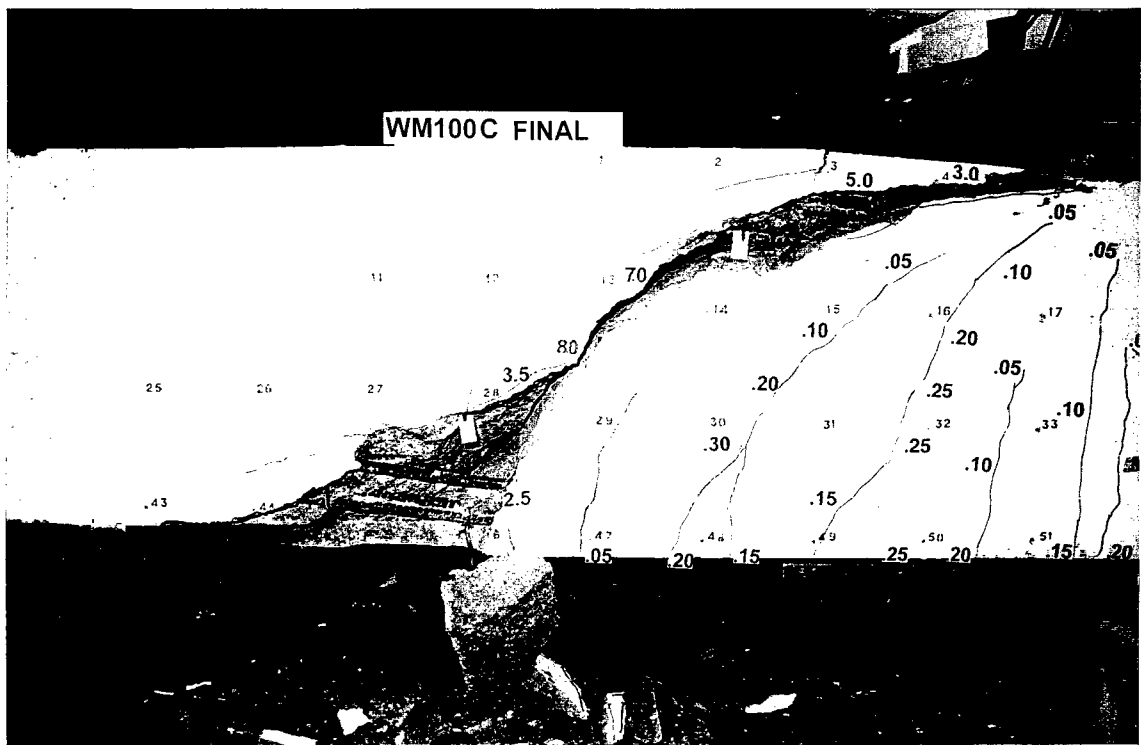


(c) Shear Stress = 0.699 MPa; Drift = 0.36%

Figure 4.3 Crack Patterns and Measured Crack Widths (mm) for Specimen WM100C



(d) Shear Stress = 0.684 MPa; Drift = 0.48%



(e) Shear Stress = 0.29 MPa; Drift = 1.06%

Figure 4.3 Crack Patterns and Measured Crack Widths (mm) for Specimen WM100C (continued)

WM100D in that the 20 longitudinal bars were clustered in the corners. For WM100D the average crack spacing, s_x , as given by Eq. (2.6) is

$$\begin{aligned} s_x &= s_{\max} + 0.1 d_{bx} / \rho_x \\ &= 0.5 \times 867 + 0.1 \times 30 / 0.014 \\ &= 434 + 214 = 648 \text{ mm} \end{aligned}$$

For the clustered pattern of reinforcing bars in WM100C, the maximum distance of the concrete in the shear area from an x -direction bar increases from 434 mm to 535 mm. See Fig. 4.1. Because 3 bars are bundled in each corner, the effective bar diameter is also increased. On the basis of the ratio of bar area to outside perimeter, the effective bar diameter, d_{beff} , of a bundle of n bars, each with a diameter of d_b is

$$\begin{aligned} d_{\text{beff}} &= \frac{d_b}{\frac{1}{\pi} + \frac{1}{n}} \quad (4.1) \\ &= \frac{30}{\frac{1}{\pi} + \frac{1}{3}} = 1.535 \times 30 = 46 \text{ mm} \end{aligned}$$

Hence, the calculated average crack spacing, s_x , for WM100C is

$$\begin{aligned} s_x &= 535 + 0.1 \times 46 / 0.014 \\ &= 535 + 329 = 864 \text{ mm} \end{aligned}$$

Because the cracks in WM100C are predicted to be more widely spaced than those in WM100D, for a given value of strain the crack widths in WM100C will be wider. Thus, it is predicted that the maximum shear that WM100C can resist will be lower than the maximum shear stress that WM100D can resist, and that this lower shear capacity will be reached at a lower deformation. The maximum shear stress resisted by WM100C was 0.699 MPa, which was 84% of the capacity of WM100D. The storey drift at this maximum load was only 0.36%, which was about one-half of the

storey drift of WM100D at its maximum load. Compare Fig. 4.3(c) and Fig. 4.2(d).

Specimen WM30C was intended to be a 30% scale model of specimen WM100C. The calculated average crack spacing, s_x , for this specimen is

$$\begin{aligned} s_x &= s_{\max} + 0.1 d_{b\text{eff}} / \rho_x \\ &= 0.5 \times 311 + 0.1 \times 1.535 \times 6.6 / 0.0137 \\ &= 156 + 74 = 229 \text{ mm} \end{aligned}$$

Figure 4.4 shows 4 stages during the test of WM30C. It can be seen that, as expected, WM30C could resist a much higher shear stress than WM100C (in fact, 49% higher) and that the storey drift at the maximum shear stress was much higher (0.71% for WM30C compared to 0.36% for WM100C). By comparing Fig. 4.3(b) and Fig. 4.4(a) it is evident that for similar levels of shear stress the crack widths in WM30C are less than one-half of those in WM100C.

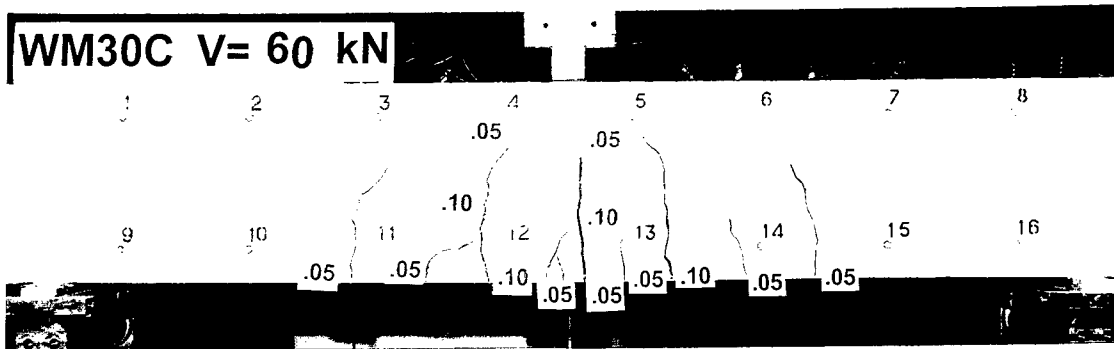
A comparison of the observed load-deformation responses of the three specimens is given in Fig. 4.5. It can be seen that, for these lightly reinforced sections, "member size", or more specifically "crack spacing" has a significant influence on the maximum shear stress that the section can resist. The line labelled ACI in Fig. 4.4 indicates the average failure shear stress according to the ACI Code[3] expression

$$V = 0.158 \sqrt{f'_c} b_w d + 17.24 \rho_w \frac{Vd}{M} b_w d + \frac{A_v f_y}{s} d \quad (4.2)$$

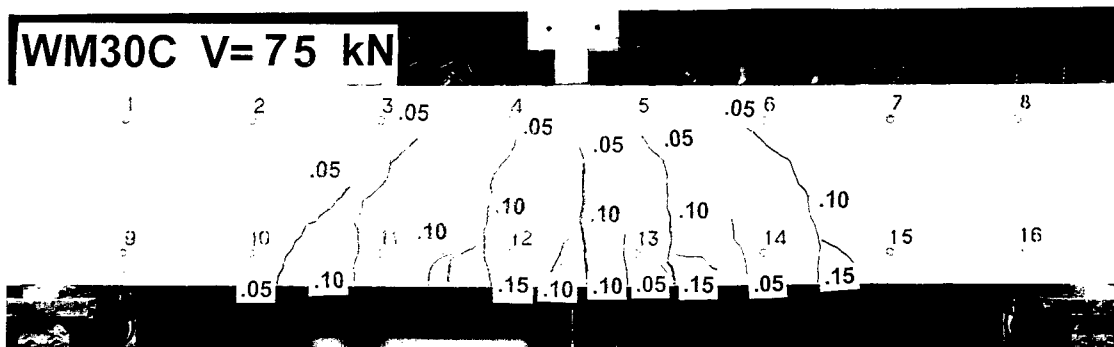
For specimen WM100C this gives

$$\begin{aligned} V &= 0.158 \sqrt{41} \times 1000 \times 925 + 17.24 \frac{7000}{1000 \times 925} \times \frac{V \times 925}{V \times 1775} \times 1000 \times 925 + \frac{2 \times 71 \times 508}{375} \times 925 \\ &= 936 + 63 + 178 = \underline{\underline{1177}} \text{ kN} \end{aligned}$$

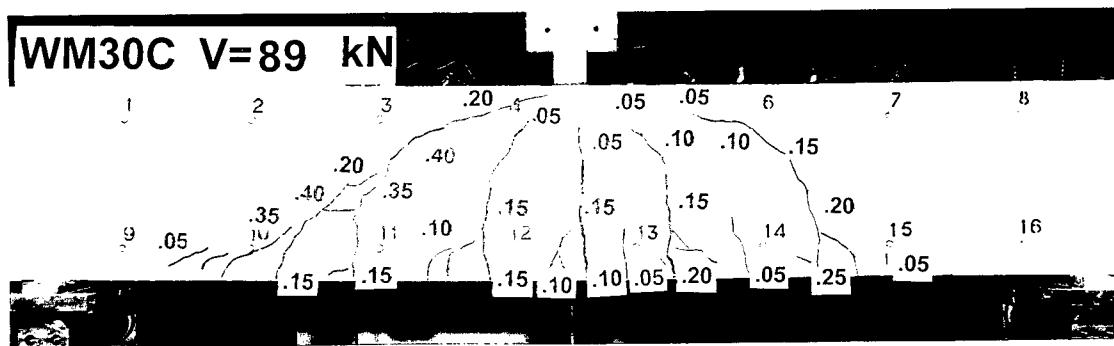
This predicted shear capacity is 168% of the actual failure shear of 699 kN, which



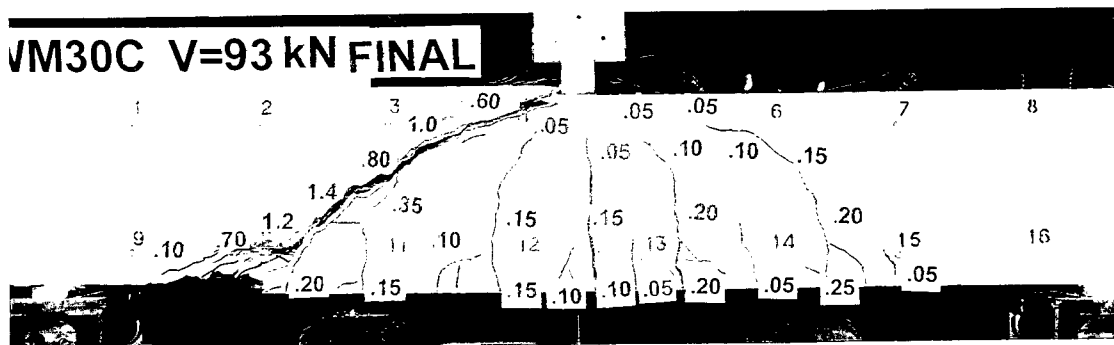
(a) Shear Stress = 0.674 MPa; Drift = 0.26%



(b) Shear Stress = 0.841 MPa; Drift = 0.39%



(c) Shear Stress = 1.000 MPa; Drift = 0.54%



(d) Shear Stress = 1.041 MPa; Drift = 0.71%

Figure 4.4 Crack Patterns and Measured Crack Widths (mm) for Specimen WM30C

indicates that the traditional shear strength expressions given in codes, e.g., Eq. (1.1), can be very unconservative indeed, for large, lightly reinforced sections.

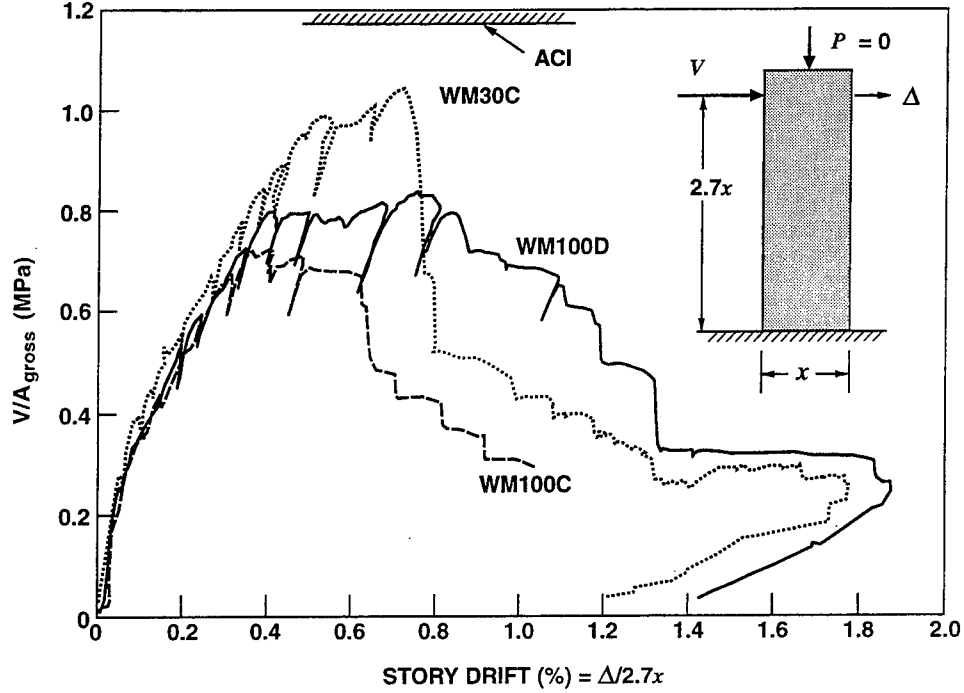


Figure 4.5 Comparison of Load-Deformation Response of WM100D, WM100C and WM30C

It is of interest to calculate the shear strength of specimen WM100C by the beta method. For such a specimen the shear stress is related to the shear force by

$$v = \frac{V}{b_v d_v} \quad (4.3)$$

where b_v is the web width and d_v is the flexural lever arm. If M_{flex} is the flexural capacity of the section when the axial load is zero and strain hardening of the reinforcement is neglected then d_v may be taken as

$$d_v = \frac{M_{flex}}{A_s f_{yield}} \quad (4.4)$$

where A_s is the area of longitudinal reinforcing bars in the flexural tension half of the cross section. For WM100C the flexural capacity is 3330 kN·m and so,

$$d_v = \frac{3330 \times 10^6}{10 \times 700 \times 550} = \underline{\underline{865}} \text{ mm}$$

As the amount of transverse reinforcement is much less than the minimum ($\rho_y f_{\text{yield}} = 0.192 \text{ MPa}$) Table 3.2 will be used to determine β and θ . For WM100C the crack spacing s_x was calculated to be 864 mm. As the maximum aggregate size was only 10 mm an equivalent spacing must be calculated from Eq. (3.2).

$$s_{xe} = \frac{35}{10 + 16} \times 864 = 1163 \text{ mm}$$

If we assume that at failure the value of ϵ_x will be 1×10^{-3} then, from Table 3.2, we can interpolate between the values for spacings of 1000 mm and 2000 mm to calculate a β value of 0.112 and a θ value of 57.6° . Hence, from Eq. (3.1)

$$\begin{aligned} v_{\max} &= 0.112\sqrt{41} + 0.192 \cot 57.6^\circ \\ &= 0.720 + 0.122 = 0.842 \text{ MPa} \end{aligned}$$

which corresponds to a shear force of

$$V_{\max} = 0.842 \times 1000 \times 865 = \underline{\underline{728}} \text{ kN}$$

The AASHTO specifications suggest that, for this type of member, the strain ϵ_x be calculated as

$$\epsilon_x = \frac{0.5V\cot\theta + 0.5N + M/d_v}{E_s A_s} \quad (4.5)$$

For a given value of ϵ_x , and known values of the shear force, V , and the axial tension, N , the above equation can be rearranged to find the corresponding value of the moment, M . Thus,

$$\begin{aligned} M &= (E_s A_s \epsilon_x - 0.5N - 0.5V\cot\theta) d_v \\ &= (200 \times 10^3 \times 10 \times 700 \times 1 \times 10^{-3} - 0 - 0.5 \times 728 \times 10^3 \cot 57.6) 865 \\ &= \underline{\underline{1011}} \text{ kN}\cdot\text{m} \end{aligned} \quad (4.6)$$

Hence, at the section where ϵ_x equals 1×10^{-3} at failure, the ratio M/V equals $1011/728$, which is 1.39 m. At the critical section d_v from the loading plate, see Fig. 4.1, the ratio M/V equals 1.76 m. As the ratio M/V increases, ϵ_x increases. If the above calculations are repeated for ϵ_x equal to 1.5×10^{-3} , V_{\max} is reduced to 588 kN and M/V is increased to 2.85 m. Interpolating between these two values, the calculated failure shear when M/V equals 1.76 m is

$$\begin{aligned} V_{\max} &= 728 - (728 - 588) \frac{1.76 - 1.39}{2.85 - 1.39} \\ &= \underline{\underline{693}} \text{ kN} \end{aligned}$$

The estimates of the failure shears for the 3 specimens obtained from the ACI method and from the beta method are compared with the observed shear capacities in Table 4.1 below.

Table 4.1 Predicted Shear Capacities of Toronto Columns

Specimen	WM100D	WM100C	WM30C
Experimental Failure Shear	834 kN	699 kN	93.7 kN
ACI Prediction	1142 kN	1177 kN	105.0 kN
Beta Prediction	737 kN	693 kN	83.3 kN
Experimental/ACI	0.73	0.59	0.89
Experimental/Beta	1.13	1.01	1.12

5. ANALYTICAL STUDIES OF COLUMN SECTIONS

To identify more precisely those situations in which the size effect in shear will be important, a series of analytical studies were conducted. These studies used specimen WM100D as the base case. Using program RESPONSE from the textbook *Prestressed Concrete Structures*[12], estimates were made of the manner in which the failure shear stress would change as the cross-sectional size was first reduced from 1 m \times 1 m to 0.3 m \times 0.3 m and then increased to 3 m \times 3 m.

Figure 5.1 illustrates the manner in which the predicted maximum shear stress capacity of the 3 series of members is predicted to change as the amount of transverse reinforcement is increased. It can be seen that when the members contain no transverse reinforcement there is a pronounced size effect. In this case the 3 m \times 3 m section is predicted to fail at a shear stress that is 67% of the failure stress of the 0.3 m \times 0.3 m section. When $\rho_y f_{y\text{ield}}$ is greater than about 0.25 MPa, the 3 m \times 3 m sections are predicted to fail at the same shear stress as the 1 m \times 1 m sections. For the 1 m \times 1 m sections the predicted value of the tension in the cracked concrete has been reduced to nearly zero and hence, further increases in section size cause no reduction in shear capacity.

Because the members shown in Fig. 5.1 contain only 1.4% of longitudinal reinforcement (i.e., 0.7% of flexural tension reinforcement) and are relatively slender (i.e., shear span to effective depth ratio equals about 3) it takes only a small amount of transverse reinforcement to ensure that they fail in flexure rather than shear. For

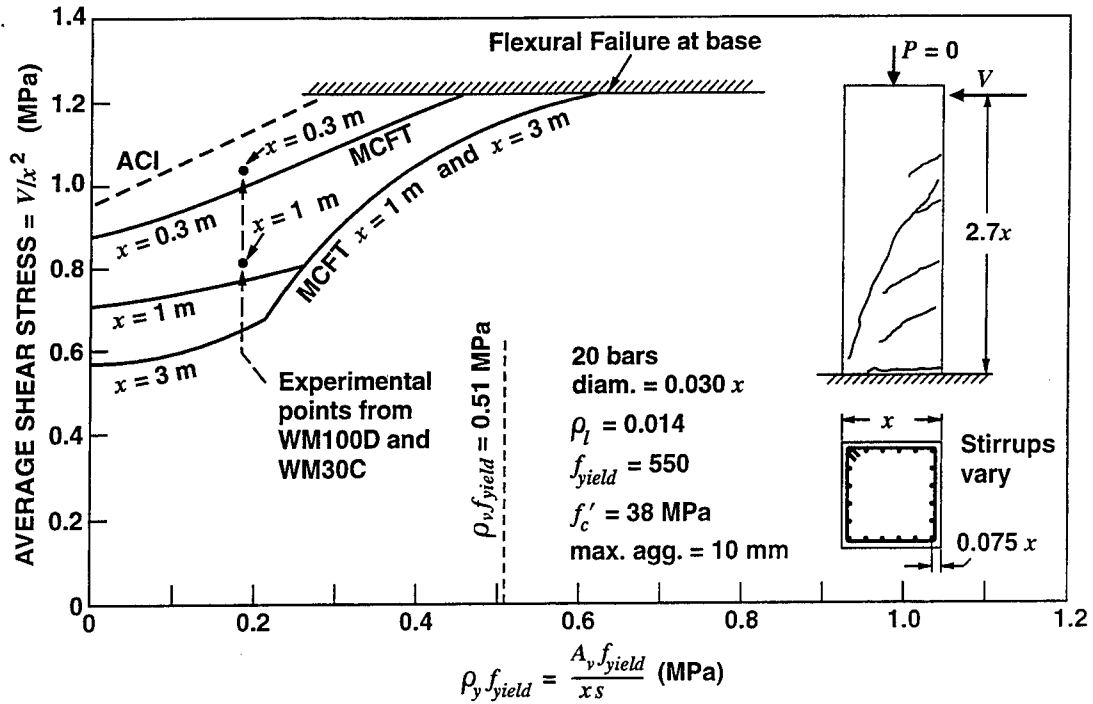


Figure 5.1 Influence of Amount of Transverse Reinforcement and Member Size on Predicted Shear Stress at Failure for Members with 1.4% of Longitudinal Steel

the $0.3 \text{ m} \times 0.3 \text{ m}$ sections the modified compression field theory (mcft) predicts that a $\rho_y f_{yield}$ value of about 0.45 MPa is required to suppress shear failures, while for the larger sections a value of about 0.62 MPa is required. The ACI equations suggest that a $\rho_y f_{yield}$ value of just 0.28 MPa will be sufficient to avoid shear failures for all three sizes. In view of the experimental result of WM100D it seems clear that this very small amount of transverse reinforcement would not suppress shear failures in the larger specimens.

It is obvious that members that contain larger amounts of longitudinal reinforcement will need to contain larger amounts of transverse reinforcement, if it is desired to have the member fail in flexure before it fails in shear. Thus the members shown in Fig. 5.2, which contain 3.0% of longitudinal reinforcement need to have a $\rho_y f_{yield}$ value of more than 1.13 MPa if shear failures are to be avoided. With this relatively large quantity of transverse reinforcement the size effect in shear is negligible.

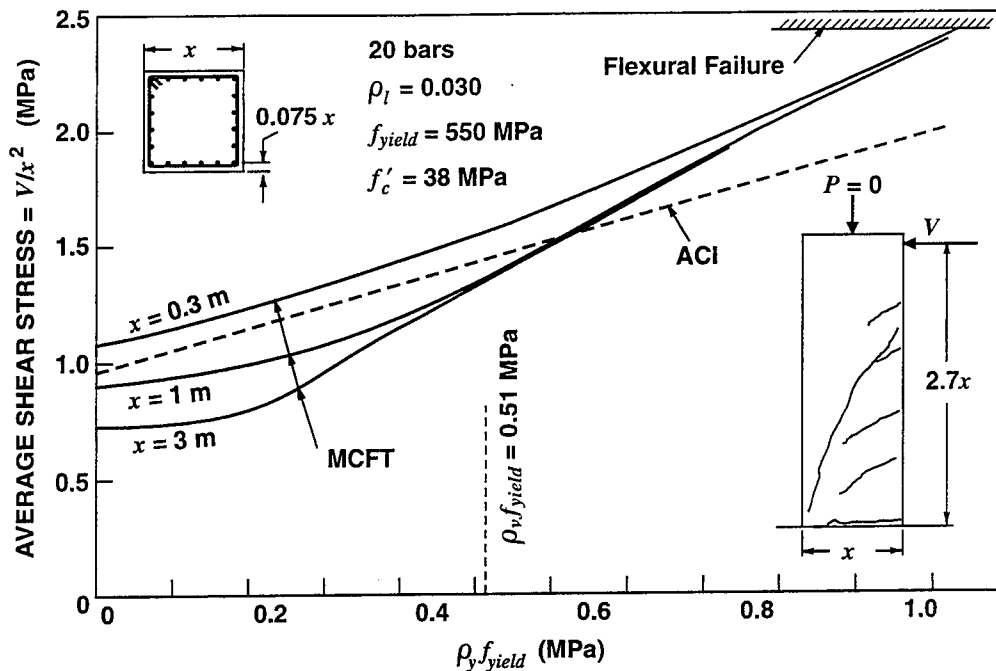


Figure 5.2 Influence of Amount of Transverse Reinforcement and Member Size on Predicted Shear Stress at Failure for Members with 3% of Longitudinal Reinforcement

Figure 5.3 illustrates the manner in which the axial load on a column will influence the predicted failure shear stress and the size effect in shear. It can be seen that, as expected, the shear capacity is predicted to increase when axial compression acts on the column, and to decrease when axial tension acts on the column. Note that the ACI Code[3] equations predict that the shear strength decreases very rapidly as axial tension is applied. As discussed in the introduction, these equations were developed at a time when it was believed that it was axial tension that caused the 0.9 m deep Air Force warehouse beams to fail at such low shear stresses. Figure 5.3 shows that as the axial compressive stress on the columns increases, the size effect in shear becomes less important. For these particular members the size effect is predicted to become negligible for compressive stresses greater than 6 MPa.

The three column tests already discussed and the analytical studies summarized in Figs. 5.1, 5.2 and 5.3, all dealt with members in which the distance

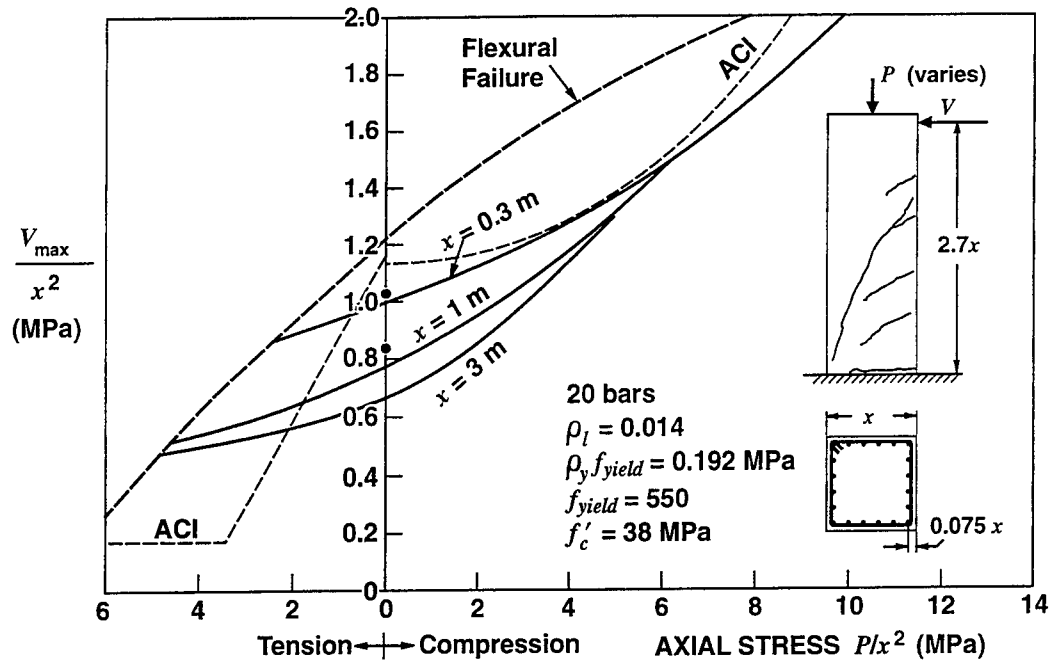


Figure 5.3 Influence of Axial Load and Member Size on Predicted Shear Stress at Failure

from the load to the support was 2.7 times the width of the square cross section. The question that then arises is how will the size effect in shear change as this aspect ratio of 2.7 changes. Figure 5.4 summarizes the results of a study in which the maximum shear stress was calculated for three series of columns ($x = 0.3$ m, $x = 1.0$ m, and $x = 3.0$ m) with aspect ratios varying from 1 to 4. Note that there are two different types of predictions shown in Fig. 5.4, namely predictions based on a sectional model and predictions based on a strut-and-tie model.

The AASHTO-LRFD specifications[14] give the details for both a sectional model for shear and a strut-and-tie model for shear. They state that the sectional model, which is the beta method discussed above, is appropriate for regions where the assumptions of traditional engineering beam theory are valid. This theory assumes that plane sections remain plane, that the shear flow is reasonably uniform over the flexural depth of the member, and that the response does not depend on the specific details of how the force effects were introduced into the member.

According to St. Venant's principle, these assumptions are only likely to be valid in

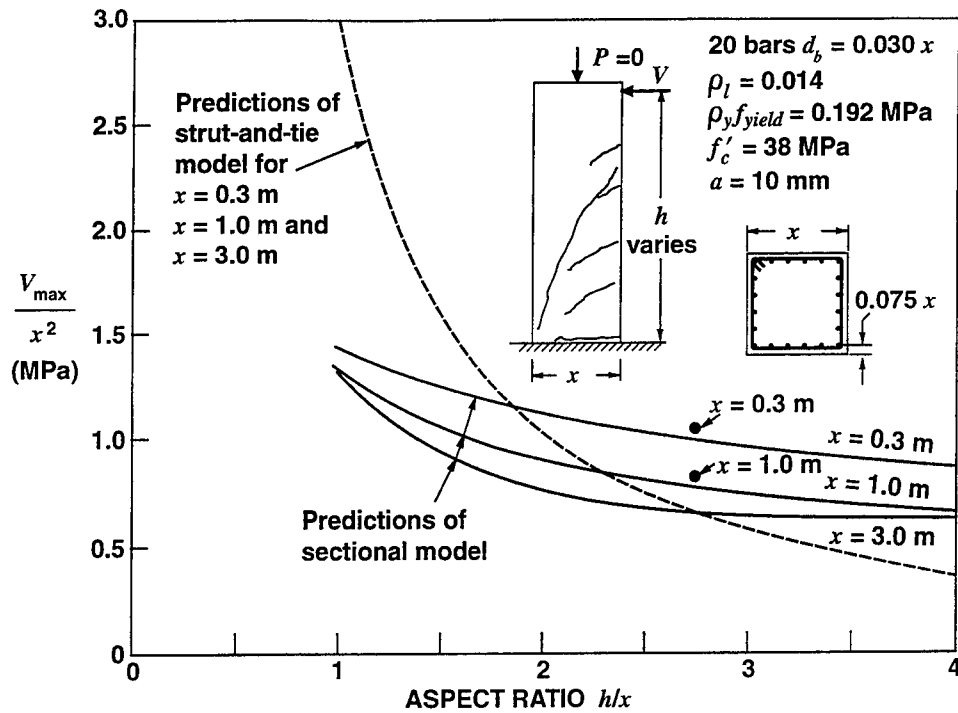


Figure 5.4 Influence of Aspect Ratio and Member Size on Predicted Shear Stress at Failure

regions that are at least a distance equal to the flexural depth of the member away from point loads or supports. For regions near such discontinuities the strut-and-tie model, which considers the actual flow of forces in the whole member in more detail, should be used.

The use of the sectional model and the strut-and-tie model is illustrated in Fig. 5.5, which compares the observed and predicted shear strengths for a series of beams tested by Kani[17]. Note that in this figure the symbol " a " is used to represent the distance from the load to the support. For a/d ratios less than about 2.5 the load carrying capacity of the "strut-and-tie" mechanism is greater than the load carrying capacity of the "sectional" mechanism. For these short beams, failure will not occur when the diagonal cracks first widen and the "sectional" capacity peaks. An internal redistribution of stresses will occur as the tensile stresses in the cracked concrete drop to near zero and the short beam begins to carry the load as a tied arch. For the members in Fig. 5.5, which had a/d ratios greater than about 2.5, the residual capacity of the "tied arch" as predicted by the strut-and-tie model is less

than the capacity of the "beam" as predicted by the sectional model. For these cases the members are predicted to fail as soon as the diagonal cracks widen. Thus, the predicted capacity of a member can be taken as the greater of the capacity predicted by the sectional model and the capacity predicted by the strut-and-tie model.

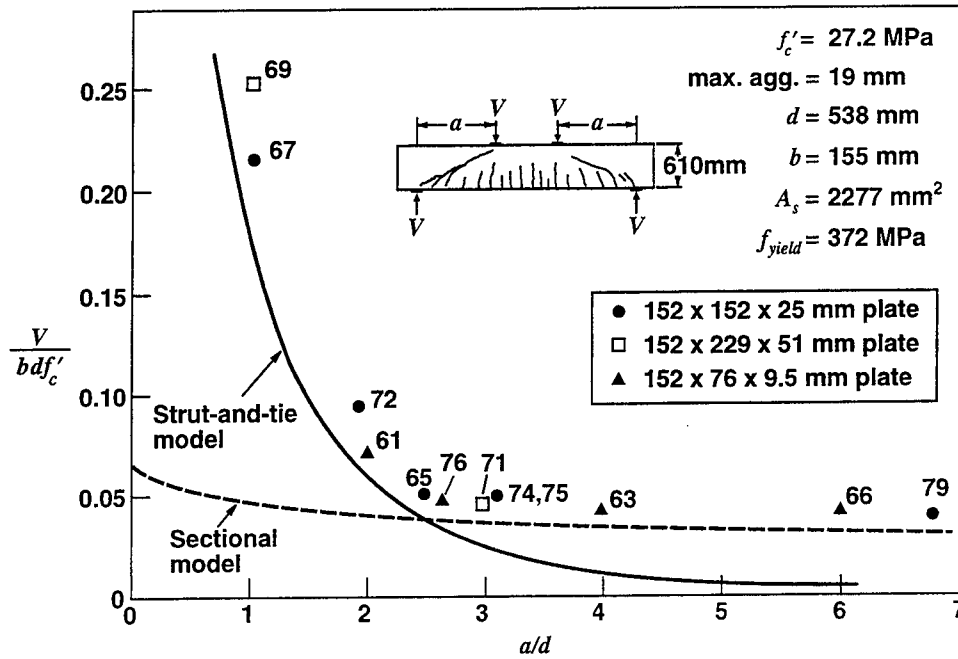


Figure 5.5 Predicted and Observed Strengths of a Series of Reinforced Concrete Beams Tested by Kani

Strut-and-tie models for the 1 m × 1 m column with aspect ratios of 1.5, 2.0 and 3.5 are shown in Fig. 5.6. As an example we will consider the model for an aspect ratio of 2.0. The longitudinal reinforcement, 20 - 30 mm bars, is clustered in the two vertical members AE and BF, each of which thus contains 10 bars. The transverse reinforcement is concentrated in the horizontal members AB, CD and EF. Member CD thus contains the transverse reinforcement from a length of 1000 mm of the column; that is, $142 \times 1000/375 = 379 \text{ mm}^2$. When this reinforcement yields, the tension force in member CD will be 379×508 , which is 192 kN. This tension force will be balanced by the 296 kN compression force in strut CB, which in turn will support 192 kN of the horizontal load applied at B. The remaining 823 kN of load is supported by strut EB, which thus has a compression force of 2106 kN.

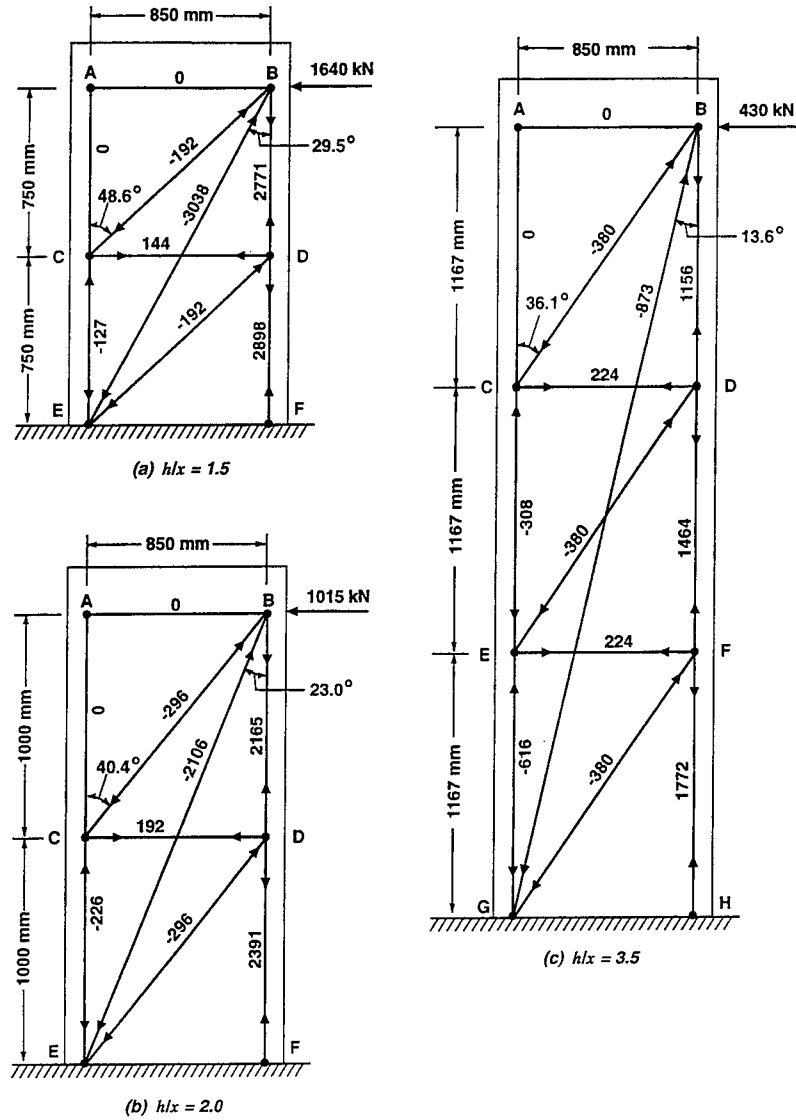


Figure 5.6 Strut-and-Tie Models for Columns with Different Aspect Ratios, Showing Member Forces (kN)

The cross-sectional area of strut EB, which is loaded by a bearing plate 150 mm long and is anchored by reinforcement 75 mm from the face of the member, can be taken[13,14] as

$$\begin{aligned}
 A_{cs} &= 1000 \times (150 \sin 23.0^\circ + 2 \times 75 \cos 23.0^\circ) \\
 &= 197000 \text{ mm}^2
 \end{aligned}$$

The limiting compressive stress in such a strut is estimated as

$$f_{cu} = \frac{f'_c}{0.8 + 170\varepsilon_1} \quad (5.1)$$

where ε_1 is the principal tensile strain to which the strut is subjected. At B, tie BD will be subjected to a tensile strain of

$$\varepsilon_s = \frac{2165 \times 10^3}{10 \times 700 \times 200 \times 10^3} = 1.55 \times 10^{-3}$$

This strain will be reduced to zero as the tie is anchored across the strut. Hence, the average tensile strain is about 0.77×10^{-3} . Assuming that the crushing strain of the strut is 2×10^{-3} the value of ε_1 is

$$\begin{aligned} \varepsilon_1 &= \varepsilon_s + (\varepsilon_s + 0.002) \cot^2 \alpha_s \\ &= 0.77 \times 10^{-3} + 2.77 \times 10^{-3} \cot^2 23.0^\circ \\ &= 16.1 \times 10^{-3} \end{aligned} \quad (5.2)$$

Hence,

$$f_{cu} = \frac{38}{0.8 + 170 \times 0.0161} = 10.72 \text{ MPa}$$

Thus, the crushing capacity of strut EB

$$\begin{aligned} P_u &= A_{cs} f_{cu} \\ &= 197000 \times 10.72 = 2110 \text{ kN} \end{aligned} \quad (5.3)$$

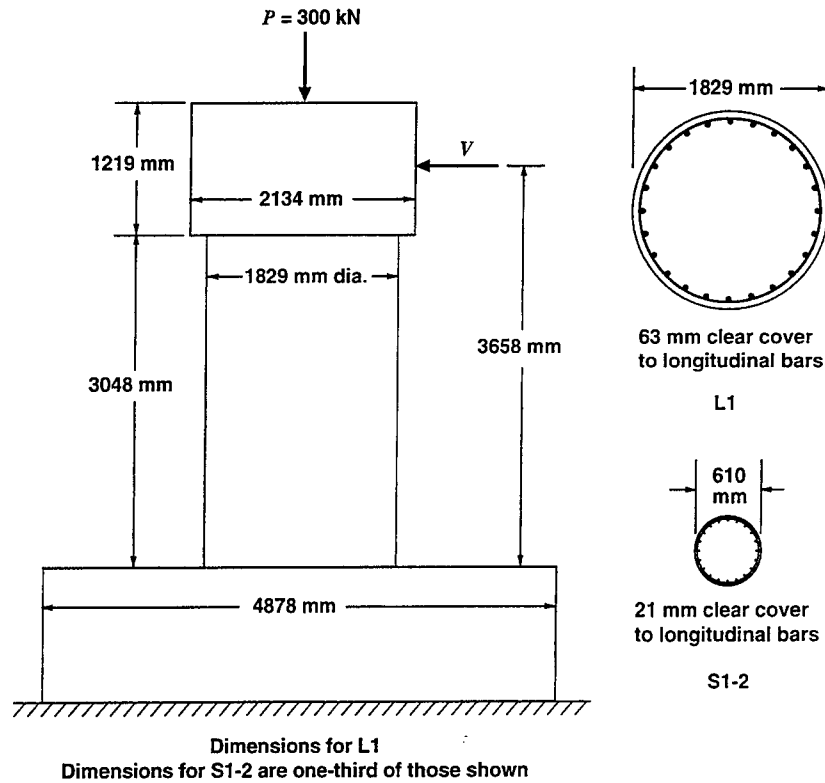
As the calculated compression force in the strut is 2106 kN, the strut is just about to crush and hence, 1015 kN is the maximum load that can be applied, according to the strut-and-tie model. Thus, for an aspect ratio of 2.0 we predict an average shear stress at failure of 1.015 MPa by the strut-and-tie model. Note that because these calculations do not involve tensile stresses in the concrete or shear stresses on crack

surfaces, there is no "size effect". Hence, the same failure shear stress is predicted for the $0.3 \text{ m} \times 0.3 \text{ m}$ columns as for the $1.0 \text{ m} \times 1.0 \text{ m}$ columns and the $3 \text{ m} \times 3 \text{ m}$ columns. See Fig. 5.4.

Because the shear capacity has no size effect for the strut-and-tie model but does have a size effect for the sectional model, the aspect ratio at which strut action begins to dominate changes with member size. Thus, for the members in Fig. 5.4, strut action dominates for aspect ratios less than 1.85 for the $0.3 \text{ m} \times 0.3 \text{ m}$ sections, less than 2.25 for the $1.0 \text{ m} \times 1.0 \text{ m}$ sections and less than 2.72 for the $3.0 \text{ m} \times 3.0 \text{ m}$ sections. The presence of strut action greatly reduces the importance of the size effect in shear for members with aspect ratios less than about 2.3. Thus, at an aspect ratio of 2.0, the predicted reduction in shear stress, as the member size is increased from $0.3 \text{ m} \times 0.3 \text{ m}$ to $3 \text{ m} \times 3 \text{ m}$, is only 10%, rather than the 33% predicted by the section model.

6. COLUMN TESTS AT THE UNIVERSITY OF CALIFORNIA, SAN DIEGO

As part of a study to investigate the influence of the size effect in shear for circular reinforced concrete columns, a 6 ft (1829 mm) diameter column, L1, and a companion 2 ft (610 mm) diameter column, S1-2, were tested under reversed cyclic loading at the University of California, San Diego in the summer of 1996. See Fig. 6.1. The columns were subjected to a small, constant axial force which caused an axial compressive stress of about 0.11 MPa. The specimens contained about 1.3% of longitudinal reinforcement and a small amount of transverse reinforcement such that $\rho_y f_{\text{yield}}$ equalled about 0.13 MPa. The specimens were loaded in single curvature such that the ratio of shear span to overall depth was 2.0. For this aspect ratio, Fig. 5.4 suggests that strut action may govern the shear capacity of the columns, being particularly important for specimen L1. It is thus of interest to calculate the shear capacity of these members using both a sectional model (i.e., the beta method) and the strut-and-tie model.



Specimen	L1	S1-2
Concrete	$f'_c = 29.6 \text{ MPa}$ $a = 25 \text{ mm}$	$f'_c = 31.2 \text{ MPa}$ $a = 25 \text{ mm}$
Longitudinal Reinforcement	24 - 43 mm bars $f_{xyield} = 508 \text{ MPa}$ $\rho_x = 0.0133$	20 - 15.9 mm bars $f_{xyield} = 454 \text{ MPa}$ $\rho_x = 0.0137$
Transverse Reinforcement	12.8 mm bars at 305 mm spacing $f_{yyield} = 298 \text{ MPa}$ $\rho_y f_{yyield} = 0.137 \text{ MPa}$	4.9 mm bars at 102 mm spacing $f_{yyield} = 210 \text{ MPa}$ $\rho_y f_{yyield} = 0.126 \text{ MPa}$

Figure 6.1 Details of Specimens Tested at University of California, San Diego

In applying the beta method to a circular section it is appropriate to calculate the shear stress, v , and the longitudinal strain, ϵ_x at the middle of the member. See Fig. 6.2. Thus,

$$v = \frac{V}{bd_v} \quad (6.1)$$

and

$$\epsilon_x = \frac{0.5V\cot\theta + 0.5N + 0.33M/d_v}{E_s A_s} \quad (6.2)$$

Further, for such a member, the average crack spacing, s_x , in the shear area can be taken as

$$s_x = \left(\frac{1}{3} + \frac{2\pi}{3n} \right) D_x + 0.1 d_{bx} / \rho_x \quad (6.3)$$

where n is the number of longitudinal bars and D_x is the diameter of the circle passing through the centres of the longitudinal bars. Thus, for specimen L1

$$\begin{aligned} s_x &= \left(\frac{1}{3} + \frac{2\pi}{3 \times 24} \right) 1660 + 0.1 \times 43 / 0.0133 \\ &= 698 + 323 = 1021 \text{ mm} \end{aligned}$$

As the maximum aggregate size was 25.4 mm this crack spacing needs to be transformed to an equivalent spacing for 19 mm aggregate before Table 3.2 can be used. From Eq. (3.2)

$$s_{xe} = \frac{35}{25.4 + 16} \times 1021 = 864 \text{ mm}$$

The calculated flexural capacity, M_{flex} , when the axial load is zero and strain hardening of the reinforcement is neglected is 12615 kN. Hence, from Eq. (4.4)

$$d_v = \frac{12615 \times 10^6}{12 \times 1452 \times 508} = 1425 \text{ mm}$$

If we assume that, at failure, the value of ϵ_x will be 0.5×10^{-3} , then, from Table 3.2, we can interpolate between the values for crack spacings of 500 mm and 1000 mm to calculate a β value of 0.173 and a θ value of 48.8° . Thus, from Eq. (3.1)

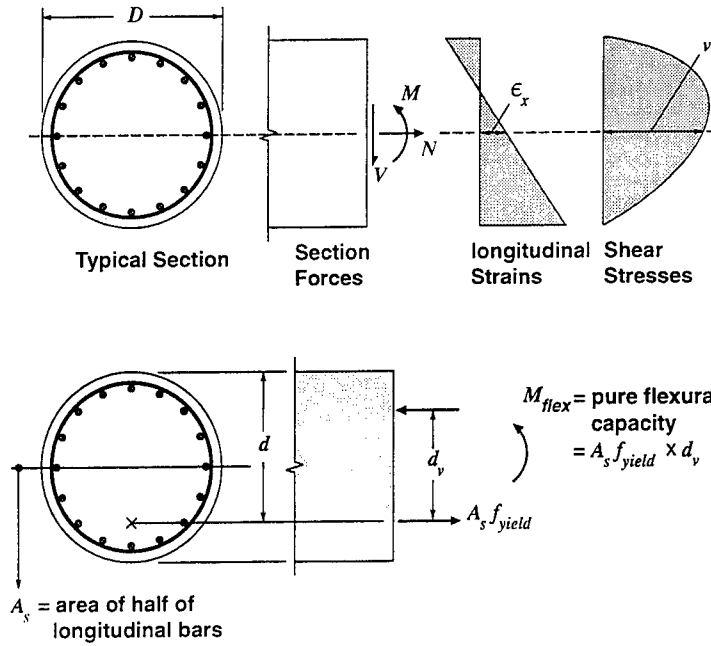


Figure 6.2 Application of the Beta Method to Circular Cross Sections

$$\begin{aligned}
 v_{\max} &= 0.173\sqrt{296} + 0.137\cot 48.8^\circ \\
 &= 0.941 + 0.120 = 1.061 \text{ MPa}
 \end{aligned}$$

which, from Eq. (6.1) corresponds to a shear force of

$$V_{\max} = 1.061 \times 1829 \times 1425 = \underline{\underline{2766 \text{ kN}}}$$

The bending moment that will correspond to these values of ϵ_x , V and θ can be found by rearranging Eq. (6.2) as

$$\begin{aligned}
 M &= 3d_v(E_s A_s \epsilon_x - 0.5N - 0.5V\cot\theta) \quad (6.4) \\
 &= 3 \times 1425(200 \times 10^3 \times 12 \times 1452 \times 0.5 \times 10^{-3} + 0.5 \times 300 \times 10^3 - 0.5 \times 2766 \times 10^3 \cot 48.8^\circ) \\
 &= \underline{\underline{2914 \text{ kN}}}
 \end{aligned}$$

Hence, at the section where, at failure, ϵ_x equals 0.5×10^{-3} the moment-to-shear ratio equals $2914/2766$, which is 1.05 m. At the critical section, which is a

distance of d_v up from the footing, the ratio M/V equals $3.658 - 1.425$, which is 2.23 m. If the above calculations are repeated for ϵ_x equal to 1.0×10^{-3} , V_{\max} is reduced to 2069 kN and M/V is increased to 5.95 m. Interpolating between these two values, the calculated failure shear of member L1, by the beta method, is

$$\begin{aligned} V_{\max} &= 2766 - (2766 - 2069) \frac{2.23 - 1.05}{5.95 - 1.05} \\ &= \underline{\underline{2598 \text{ kN}}} \end{aligned}$$

An appropriate strut-and-tie model for column L1 is shown in Fig. 6.3. The 24 longitudinal bars are clustered in the two vertical members AF and BG, each of which thus contains 12 bars. These vertical members are spaced apart a distance equal to the flexural lever arm, d_v . The transverse reinforcement within a distance of 1524 mm is concentrated in horizontal member CD, which thus contains $257 \times 1524/305 = 1284 \text{ mm}^2$. When this reinforcement yields, the tension force in member CD will be $1284 \times 298 = 383 \text{ kN}$. This tension force will be balanced by the 692 kN compression force in strut DA, which in turn will support 383 kN of the horizontal force applied at A. The remaining 2717 kN of applied load is supported by strut AE, which thus has a compressive force of 7758 kN .

The cross-sectional area of strut AE near the top of the circular column can be estimated from the section shown in Fig. 6.3 as

$$A_{cs} = 1535 \times 810 = 1.243 \text{ m}^2$$

The tensile strain in tie AC can be estimated as

$$\epsilon_s = \frac{7690 \times 10^3}{12 \times 1452 \times 200 \times 10^3} = 2.21 \times 10^{-3}$$

This strain will be reduced to zero as the tie is anchored across the strut. Hence, the average tensile strain in the vertical direction in the strut is about 1.10×10^{-3} .

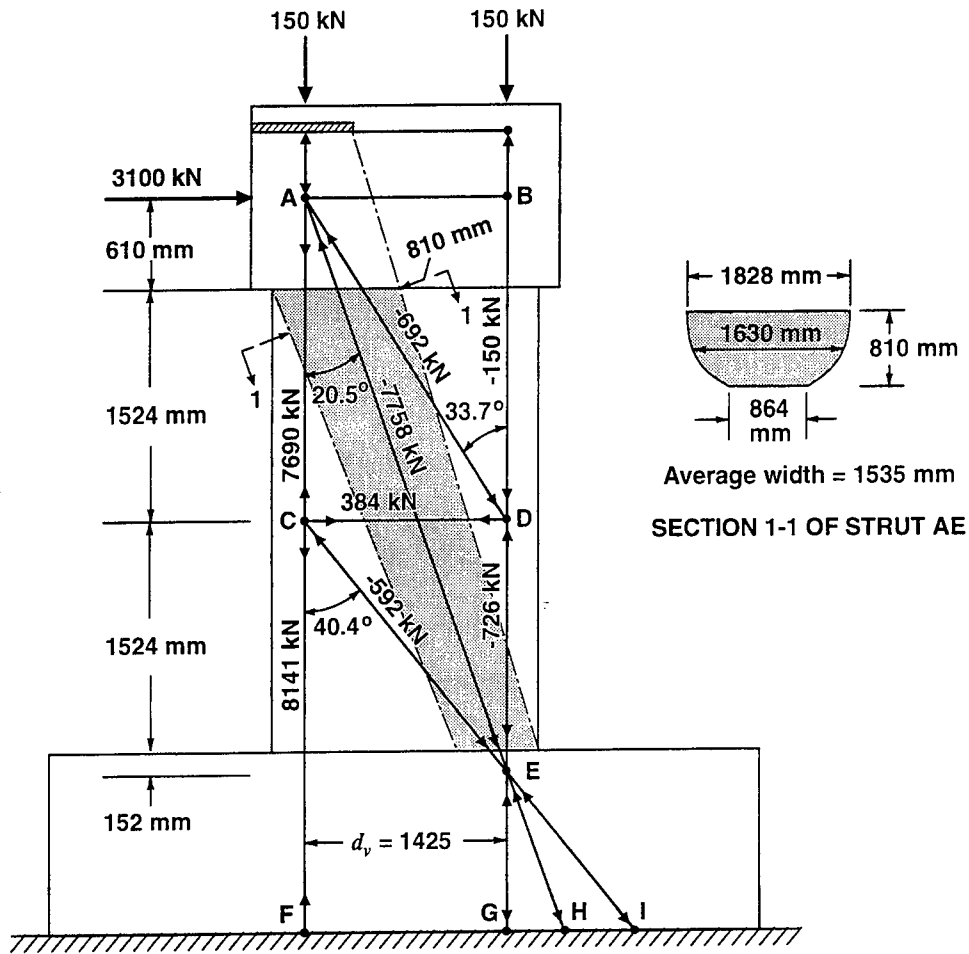


Figure 6.3 Strut-and-Tie Model of Column L1

Assuming that the crushing strain of the strut is 2×10^{-3} , the value of ϵ_1 perpendicular to the strut is

$$\begin{aligned}\epsilon_1 &= 1.10 \times 10^{-3} + (1.10 \times 10^{-3} + 2.0 \times 10^{-3}) \cot^2 20^\circ \\ &= 23.3 \times 10^{-3}\end{aligned}$$

The predicted crushing stress of the strut is found from Eq. (5.1) as

$$f_{cu} = \frac{29.6}{0.8 + 170 \times 23.3 \times 10^{-3}} = 6.22 \text{ MPa}$$

Thus, the crushing capacity of strut AE is predicted to be

$$\begin{aligned}
 P_u &= A_{cs} f_{cu} = 1.243 \times 10^6 \times 6.22 \\
 &= \underline{\underline{7740 \text{ kN}}}
 \end{aligned}$$

To reduce the compression force in strut AE to 7740 kN the applied horizontal force needs to be reduced to 3095 kN. Thus, the predicted capacity of column L1, according to the strut-and-tie model, is 3095 kN.

The predicted shear capacities of columns L1 and S1-2, according to the sectional model (beta method) and the strut-and-tie model are shown in Table 6.1 below. It can be seen that the predicted capacity from the strut-and-tie model is 19% greater than the sectional model prediction for L1 and 3% greater for S1-2. For both columns strut action is predicted to dominate and hence, the two columns are predicted to fail at about the same shear stress.

Table 6.1 lists the maximum shear force that the columns resisted during the reversed cyclic loading tests and also lists three other sets of predicted values, namely, the load at which yielding of the longitudinal reinforcement commences at the base of the column, the load causing flexural failure at the base of the column, and the failure load predicted by a non-linear finite element analysis using a program called TRIX96[18], which is based on the modified compression field theory. It will be noted that both the experimental columns and the TRIX96 analytical models fail at loads that are between the first yield loads and the flexural failure loads. Also note that, because of small differences in the geometric and material parameters, the ratio of the flexural failure load of L1 to the flexural failure load of S1-2 is 10.07 rather than the ideal value of 9.0.

In evaluating the seismic response of a bridge column the ductility of the member, as exhibited by the load-deformation response, is of equal importance with the strength. While the TRIX96 analyses predict that both the large column, L1, and the small column, S1-2, will fail at the same average shear stress, they predict that the smaller column will be more ductile. See Fig. 6.4. This result suggests that member size may affect the observed ductility in members that are shear critical.

Table 6.1 Predicted Shear Capacities of San Diego Columns

Specimen	L1	S1-2	L1/S1-2
Sectional Model	2598 kN	349 kN	7.44
Strut-and-Tie Model	3095 kN	361 kN	8.57
Predicted Capacity	3095 kN	361 kN	8.57
Experimental Failure	3104 kN	332 kN	9.35
First Yielding	2865 kN	301 kN	9.52
Flexural Failure	3835 kN	381 kN	10.07
TRIX96 Prediction	3340 kN	371 kN	9.00

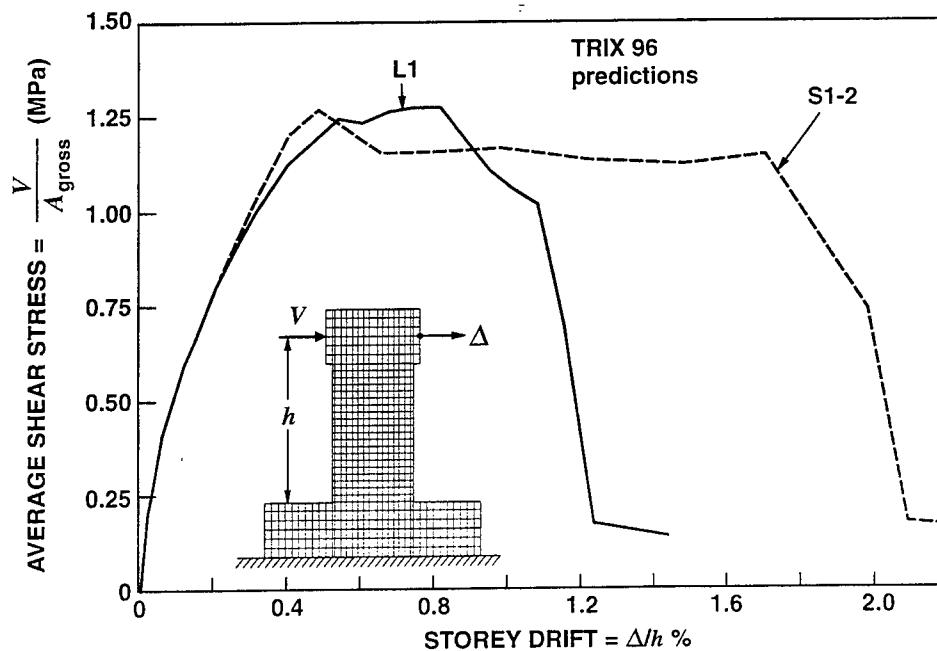


Figure 6.4 Predicted Load-Deformation Response of Columns L1 and S1-2

It was thought that the larger ductility predicted for column S1-2 may have been partly due to the fact that first flexural yielding of the longitudinal reinforcement was predicted to occur at a somewhat lower shear stress in member S1-2 than in L1. To investigate the influence of member size on the predicted load-deformation response of a series of members with identical material properties, three

analyses were performed using TRIX96. Figure 6.5 shows the predicted relationships between the applied average shear stress (i.e., shear force divided by cross-sectional area) and the resulting storey drift (i.e., deformation divided by storey height) for three columns. The middle column of the set is specimen L1, that is a 6 ft (1829 mm) diameter column. The smallest column of the set is a one-third scale model of L1, while the largest column is a version of L1 scaled up by a factor of 3; i.e., it has a diameter of 18 ft (5486 mm). Figure 6.5 shows how the resulting change of crack spacings influences the predicted load-deformation response for this type of member. It can be seen that the predicted maximum shear stress is reduced by only about 10% as the column size is increased from a 2 ft (610 mm) diameter to an 18 ft (5486 mm) diameter. While the predicted loss in ductility is small as the column size is increased from 6 ft (1829 mm) diameter to 18 ft (5486 mm) diameter, there is a substantial increase in the predicted ductility as the column size is decreased from 6 ft (1829 mm) diameter to 2 ft (610 mm) diameter.

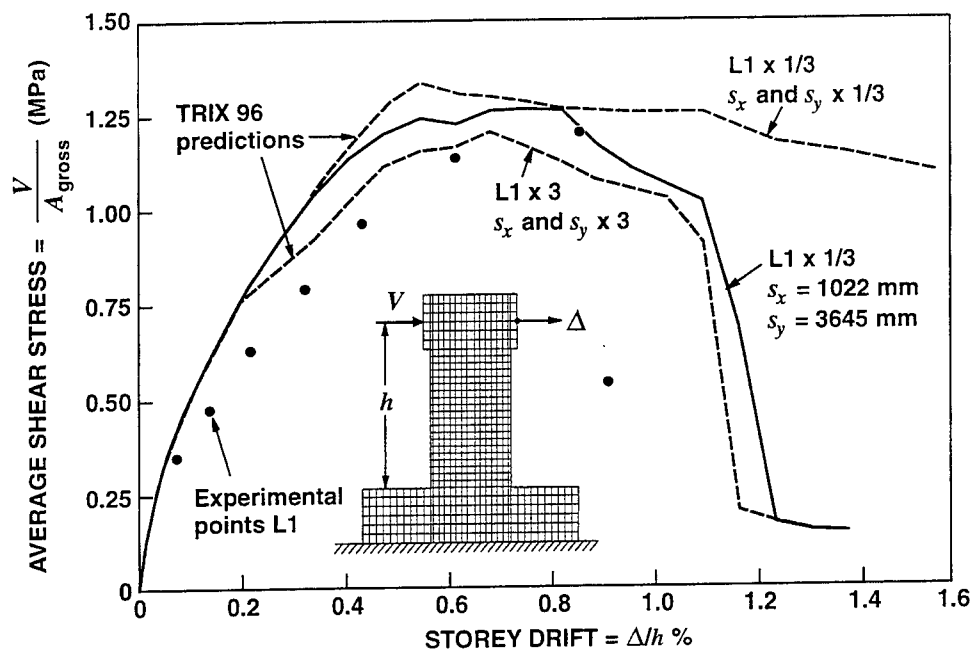


Figure 6.5 Influence of Crack Spacing on Predicted Load-Deformation Response

Figure 6.5 also enables the load-deformation response for specimen L1 predicted by TRIX96 analysis, to be compared with experimental points taken from the envelope of the measured load-deformation response. It can be seen that the analytical model underestimated somewhat the member deformations during the period when the load was being increased, but overestimated somewhat the deformation at which the capacity would suddenly drop. In view of the complexity of the actual response, and the detrimental effects of the reversed cyclic loading, which were not accounted for in the analytical model, it is believed that the agreement between the predicted and observed load-deformation responses shown in Fig. 6.5 is very satisfactory.

The predicted deformed shape of L1 at its maximum load is shown in Fig. 6.6. Note the large shear distortions in a band of elements running from the top left to the bottom right of the column. Also note that the diameter of the column has significantly increased near mid-height of the column. This "bulging" of the column is an indicator that a shear failure is imminent. The predicted crack pattern for L1 at its maximum load is shown in Fig. 6.7. The diagonal band of wide cracks also indicates a shear failure.

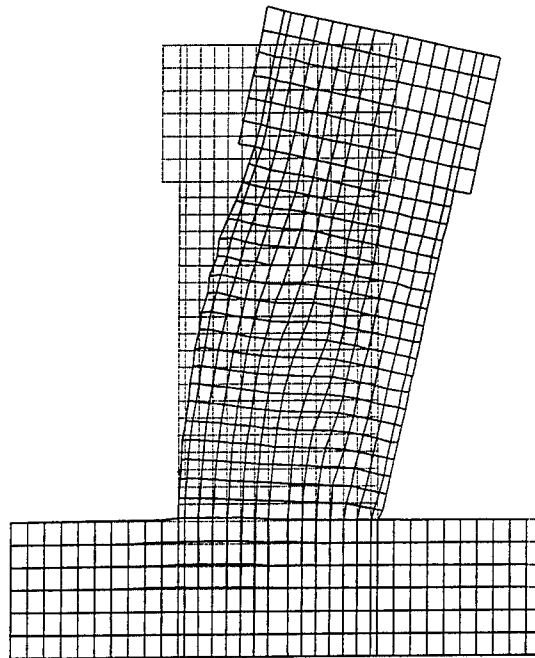


Figure 6.6 Deformed Shape of L1 under Maximum Load, Predicted by TRIX96

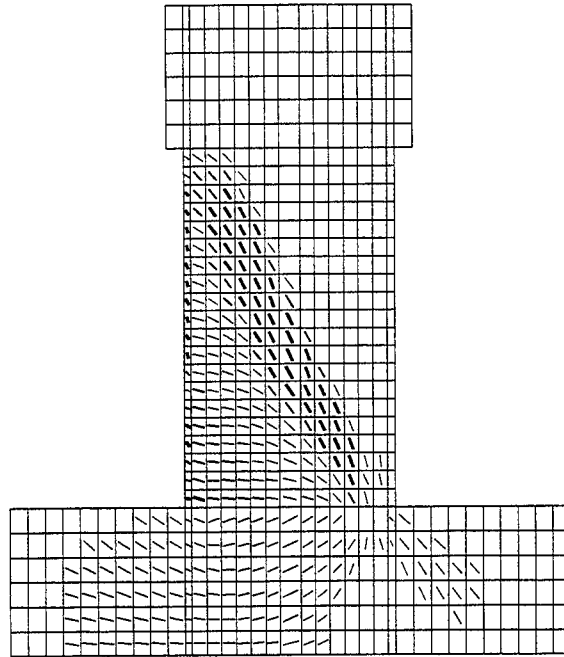


Figure 6.7 Crack Pattern for L1 under Maximum Load, Predicted by TRIX96

7. CONCLUSIONS

The experimental and analytical studies described in this report demonstrate that in many practical situations member size will influence the failure shear stress and the ductility of reinforced concrete members. Columns that contain only small amounts of shear reinforcement, are made from concrete using smaller aggregates, are subjected to low axial loads, and have ratios of column height to member thickness greater than about 2.5 are particularly sensitive to the size effect in shear. Three such columns, tested at the University of Toronto and discussed in this report, showed that the maximum shear stress that could be resisted reduced from 1.041 MPa to 0.699 MPa as the column size was increased from a 300 mm \times 300 mm section to a 1000 mm \times 1000 mm section. As well as reducing the failure shear stress, an increase in size reduced the ductility of the section. The 300 mm \times 300 mm specimen reached its peak load at a drift of 0.71%, while the 1000 mm \times 1000 mm section reached its peak load at a 0.36% drift.

Members that contain more shear reinforcement are less sensitive to the size effect in shear. Analytical studies indicate that members containing the minimum

amount of shear reinforcement given by the AASHTO-LRFD specifications may show a reduction in failure shear stress equal to about 15% as member size is increased from 300 mm \times 300 mm to 3000 mm \times 3000 mm. Members with twice this amount of shear reinforcement show only a 1.5% reduction in shear strength due to the size effect.

Columns that are subjected to significant axial compression are also less sensitive to the size effect in shear. For the members studied in this report, the size effect in shear was predicted to become negligibly small when the axial compressive stress on the column reached 6 MPa.

When the aspect ratio, defined as the ratio of the height of a column to its overall thickness, becomes small a significant portion of the applied horizontal load can be carried by a diagonal strut of concrete going from the load location down to the support. The capacity of this load carrying mechanism can be estimated using the strut-and-tie model given in the AASHTO-LRFD specifications. These specifications give both a sectional model, called the beta method, which for members containing less than the minimum amount of stirrups, incorporates a size effect, and a strut-and-tie model, which does not contain a size effect. The predicted shear capacity of a member, according to these specifications, should be taken as the larger of the shear capacities predicted by the two models. The aspect ratio at which strut-and-tie action begins to dominate changes with member size, going down from about 2.7 for 3 m members to 1.8 for 0.3 m members. The presence of strut action is predicted to greatly reduce the importance of the size effect in shear for members with aspect ratios less than about 2.3.

The sensitivity of the size effect in shear to the aspect ratio of the column can be observed if two of the column tests from the University of Toronto are compared with the two column tests from the University of California, San Diego. As can be seen in Table 7.1 below, the two sets of columns had similar percentages of longitudinal reinforcement and similar amounts of shear reinforcement. The Toronto columns, with an aspect ratio of 2.7, showed a decrease in shear stress capacity of 33% as the member size increased by a factor of 3.33. On the other

hand, the San Diego columns, which had an aspect ratio of 2.0, displayed an increase in shear stress capacity of 4% as the member size increased by a factor of 3.

Table 7.1 Comparison of Toronto and San Diego Column Tests

Test Location	Toronto		San Diego	
Specimen	WM100C	WM30C	L1	S1-2
Cross-Section	square	square	circular	circular
Section Size	1000 mm	300 mm	1829 mm	610 mm
Longitudinal Steel, ρ_x	1.40%	1.37%	1.33%	1.37%
Transverse Steel, $\rho_y f_{y\text{yield}}$	0.192 MPa	0.192 MPa	0.137 MPa	0.126 MPa
Concrete, f'_c	41 MPa	41 MPa	29.6 MPa	31.2 MPa
Aspect Ratio	2.7	2.7	2.0	2.0
Maximum Shear Stress	0.70 MPa	1.04 MPa	1.18 MPa	1.14 MPa
Ratio Large/Small	0.67		1.04	

It is shown in the report that analytical methods based on the modified compression field theory are capable of predicting reasonably well the size effect in shear. These methods include the beta model and the strut-and-tie model, which are suitable for hand calculations, program RESPONSE, which predicts the load-deformation response of a section, and program TRIX96, which conducts a non-linear finite element analysis of the complete member. Analytical studies using TRIX96 indicated that while member size has only a small influence on the failure shear stress of columns with low aspect ratios, increasing the member size can significantly reduce the ductility of these members.

It is believed that the studies summarized in this report provide guidance as to when serious consideration needs to be given to the effects of member size on the shear response of reinforced concrete members.

REFERENCES

- [1] Shioya, T., Iguro, M., Nojiri, Y., Akiyama, H., and Okada, T., "Shear Strength of Large Reinforced Concrete Beams," *Fracture Mechanics: Application to Concrete*, SP-118, American Concrete Institute, Detroit, 1989, 309 pp.
- [2] Shioya, T., "Shear Properties of Large Reinforced Concrete Member," Special Report of Institute of Technology, Shimizu Corporation, No. 25, Feb. 1989, 198 pp.
- [3] ACI Committee 318, "Building Code Requirements for Structural Concrete (ACI 318-95) and Commentary ACI 318R-95," American Concrete Institute, Detroit, 1995, 369 pp.
- [4] ACI-ASCE Committee 326, "Shear and Diagonal Tension," *ACI Journal*, V. 59, Jan., Feb., and Mar. 1962, pp. 1-30, 277-344, and 352-396.
- [5] Anderson, B.G., "Rigid Frame Failures," *ACI Journal*, V. 53, Jan. 1957, pp. 625-636.
- [6] ACI Committee 318, "Building Code Requirements for Reinforced Concrete," American Concrete Institute, Detroit, 1951.
- [7] Elstner, R.C. and Hognestad, E., "Laboratory Investigation of Rigid Frame Failure," *ACI Journal*, V. 53, Jan. 1957, pp 637-668.
- [8] Vecchio, F.J., and Collins, M.P., "The Modified Compression Field Theory for Reinforced Concrete Elements Subjected to Shear," *ACI Journal*, Vol. 83, No. 2, Mar.-Apr. 1986, pp. 219-231.
- [9] Vecchio, F.J., and Collins, M.P., "The Response of Reinforced Concrete to In-Plane Shear and Normal Stresses," Publication No. 82-03, Department of Civil Engineering, University of Toronto, Mar. 1982, 332 pp.
- [10] Bhude, S.B. and Collins, M.P., "Influence of Axial Tension on the Shear Capacity of Reinforced Concrete Members," *ACI Structural Journal*, Vol. 86, No. 5, Sept.-Oct. 1989, pp. 570-581.
- [11] Kirschner, U., and Collins, M.P., *Investigating the Behaviour of Reinforced Concrete Shell Elements*, Publication No. 86-9, Department of Civil Engineering, University of Toronto, Sept. 1986, 209 pp.

- [12] Collins, M.P., "Towards a Rational Theory for RC Members in Shear,"
Journal of the Structural Division, ASCE, Vol. 104, Apr. 1978, pp. 649-666.
- [13] Collins, M.P. and Mitchell, D., *Prestressed Concrete Structures*, Prentice Hall, Englewood Cliffs, 1991, 766 pp.
- [14] *AASHTO LRFD Bridge Design Specifications and Commentary*, First Ed., American Association of State Highway and Transportation Officials, Washington, 1994, 1091 pp.
- [15] Collins, M.P., Mitchell, D., Adebar, P.E., and Vecchio, F.J., "A General Shear Design Method," *ACI Structural Journal*, Vol. 93, No. 1, Jan-Feb 1996, pp. 36-45.
- [16] CSA Committee A23.3, *Design of Concrete Structures: Structures (Design) - A National Standard of Canada*, Canadian Standards Association, Rexdale, Dec. 1994, 199 pp.
- [17] Kani, M.W., Huggins, M.W., and Wittkopp, R.R., *Kani on Shear in Reinforced Concrete*, Department of Civil Engineering, University of Toronto, Toronto, 1979, 225 pp.
- [18] Vecchio, F.J., "Nonlinear Finite Element Analysis of Reinforced Concrete Membranes," *ACI Structural Journal*, Vol. 86, No. 1, Jan.-Feb. 1989, pp. 26-35.